

Structural Aspects of the Topochemical Polymerization of Diacetylenes

Volker Enkelmann

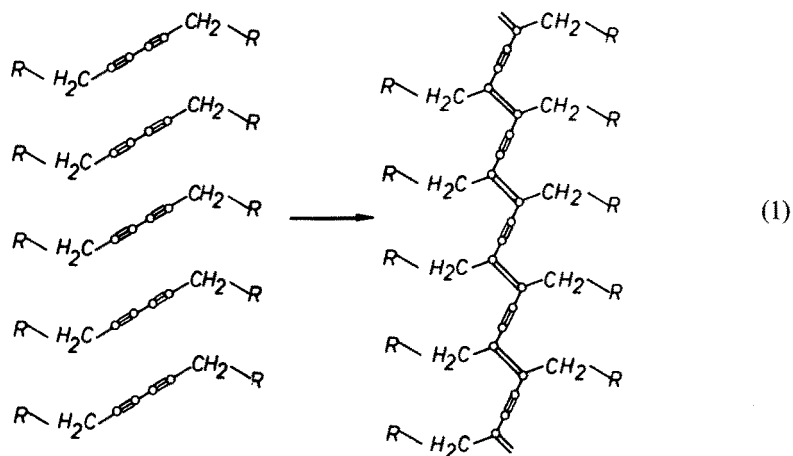
Institut für Makromolekulare Chemie, Hermann-Staudinger-Haus,
Stefan-Meier-Str. 31, 7800 Freiburg, FRG

The present state of knowledge of the topochemical polymerization of diacetylenes is reviewed with regard to structural properties. Principles and mechanisms of topochemical reactions are described. Solid-state polymerization of diacetylenes utilizes the special packing properties of monomer units in their crystals. Rules relating reactivity in the solid-state and packing properties are given and the relation between reaction mechanism, molecular mobility and polymer morphology are discussed. The growth of the macromolecules in the monomer crystal, the molecular weight and its distribution with regard to the reaction kinetics and phase transitions are outlined. The electronic structure of the polydiacetylene chain is best represented by the acetylene resonance structure consisting of alternating double, single and triple bonds.

1 Introduction	92
2 Principles of Topochemical Reactions	93
3 Structure and Reactivity	95
3.1 Packing of Diacetylene Monomers	95
3.2 Crystal Structure Analysis of Diacetylene Monomers	103
3.3 Molecular Motions Connected with the Topochemical Polymerization of Diacetylenes	105
4 Polymer Growth in the Monomer Matrix	108
4.1 Structural Investigations	108
4.2 The Crystal Strain Theory	110
4.3 Reaction Kinetics and Molecular Weight Distribution	112
5 Phase Transitions	115
5.1 Conversion Dependent Phase Transition in DCH	116
5.2 Conversion Dependent Phase Transition in PTS-12	119
5.3 The Low Temperature Phase of PTS	120
5.4 The Low Temperature Phase of DCH	123
6 Structure of the Polydiacetylene chain	126
7 Polymerization in Mixed Crystals	128
8 References	133

1 Introduction

Many examples of solid-state reactions in organic crystals already were reported in the nineteenth century. Since then a great variety of examples have been found, e.g. dimerizations, polymerizations, cis-trans isomerizations or substituent migrations. These fascinating and, at the time of their discovery inexplicable results have been only recently understood using the rapid progress of x-ray structure analysis and spectroscopic techniques. Diacetylenes have been noted for a long time to undergo drastic colour changes upon storage or exposure to light although both crystal shape and chemical analysis apparently did not change¹⁻¹¹⁾. G. Wegner demonstrated in 1969 that the solid-state polymerization of diacetylenes can be characterized as a diffusionless, totally lattice controlled process according to¹²⁾.



The principles of such topochemical reactions have been established by G. M. J. Schmidt for the dimerization of cinnamic acid derivatives which represents the other classical organic solid-state reaction^{13, 14)}.

Some important aspects of topochemical polymerizations can be understood by inspection of Eq. (1). All reactivity comes about by very specific rotations of the monomers and by 1,4-addition of adjacent units and an extended, fully conjugated polymer chain is formed. The unique feature of the topochemical polymerization of diacetylenes is the fact that in many cases the reaction can be carried out as a single phase process. This leads to macroscopic, defect-free polymer single crystals which cannot be obtained, in principle, by crystallization of ready-made polymers by conventional methods. Thus, polydiacetylenes are ideal models for the investigation of the behaviour of macromolecules in their perfect three dimensional crystal lattice.

Owing to the mechanism of the topochemical reaction the polyconjugated polymer chain is of exceptional purity and stereochemical regularity. Polydiacetylene crystals are thus ideally suited to study the inherent optical and electrical properties of polyconjugated chains. These unique features have attracted considerable attention and in recent years the topochemical polymerization of diacetylenes has developed to

one of the best investigated chemical reactions. It is therefore almost impossible to cover all developments ranging from synthetic chemistry to solid state physics.

The following is an attempt to summarize the structural data which have been accumulated recently and to critically review the present state of knowledge on the formation and structural properties of polydiacetylenes and to point out some directions of future developments in the field. Other aspects have been reviewed recently¹⁵⁻²⁵⁾ and the photopolymerization and reaction kinetics as well as the spectroscopic identification of the reactive intermediates will be covered by H. Bässler and H. Sixl^{107, 116)}.

2 Principles of Topochemical Reactions

Reactivity in the solid-state is always connected with specific motions which allow the necessary contact between the reacting groups. In most cases "solid-state" reactions proceed by diffusion of reactions to centers of reactivity or by nucleation of the product phase at certain centers of disorder. This leads to the total destruction of the parent lattice. If the product is able to crystallize it is highly probable that nucleation of the crystalline product phase at the surface of the parent lattice will lead to oriented growth under the influence of surface tension. In such "topotactic" reactions certain crystallographic directions of parent and daughter phases will coincide. Typical examples for this behaviour are the solid-state polymerizations of oxacyclic compounds such as trioxane, tetraoxane or β -propiolactone²⁶⁾.

In contrast to this behaviour a topochemical reaction can be described as a diffusionless transformation of the parent crystal into the daughter crystal. All reactivity comes about by very specific rotations of the monomers on their lattice sites. Both crystallographic position and symmetry of the monomer units are retained in this process which is schematically shown in Fig. 1.

The principles of topochemical reactions have been worked out by G. M. J. Schmidt for the example of the well known 2+2 cycloadditions of olefins, e.g. cinnamic acid derivatives¹³⁾.

As it was mentioned above the centers of the reacting molecules ideally remain fixed in topochemical reactions. As a consequence the reaction mode which requires the smallest atom displacements will prevail (least motion principle). Reactivity is

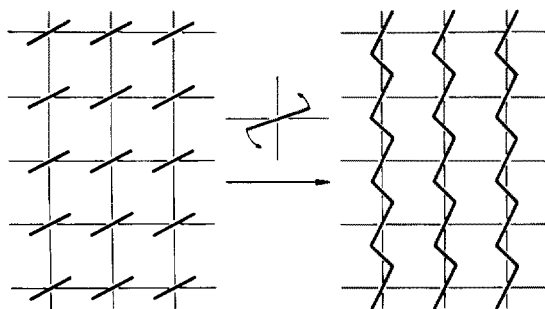


Fig. 1. Scheme of a topochemical polymerization. Transformation of a monomer single crystal into the polymer single crystal

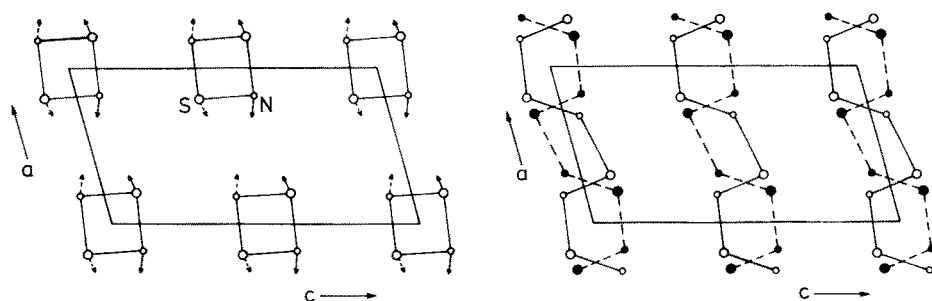


Fig. 2. Crystal structures of S_2N_2 and $(SN)_x$. The arrows in the monomer structure indicate atom displacements

only observed if the separation of the reaction atoms is less than a limiting distance of approximately 4 \AA ²²⁻²⁵). The new chemical bonds are all oriented along a specific crystallographic direction. For the case of a topochemical polymerization this means that extended chain polymers are formed.

The symmetry of the monomer packing determines the symmetry of the products, e.g. cinnamic acids will form only one of the various possible dimers, the symmetry of which is present in the monomer crystal¹³). Even absolute asymmetric syntheses are possible utilizing the symmetry relationships of topochemical reactions²⁷⁻²⁹).

Topochemical reactions can be regarded as special phase transitions. If the crystal symmetry is changed during the reaction this leads, depending on the cooperativity of the molecular motion, to order-disorder structures, twinning or phase separation. A good example where this uniqueness criterion is violated is the synthesis of $(SN)_x$. The rings of the precursor S_2N_2 are arranged in a way that two reaction modes are equally possible (Fig. 2). As a consequence, the polymer obtained consists of fibrils with typical diameters of 200 \AA ³⁰).

Apart from the uniqueness of the reaction the morphology of the product depends substantially on the distribution of the reaction centers in the crystal. Two limiting cases can be considered. In the case of a heterogeneous topochemical process the reaction starts preferentially at specific defect sites and proceeds with nucleation of product phases. This mechanism eventually leads to the destruction of the mother crystal since the coherence between the various nuclei is lost under the influence of

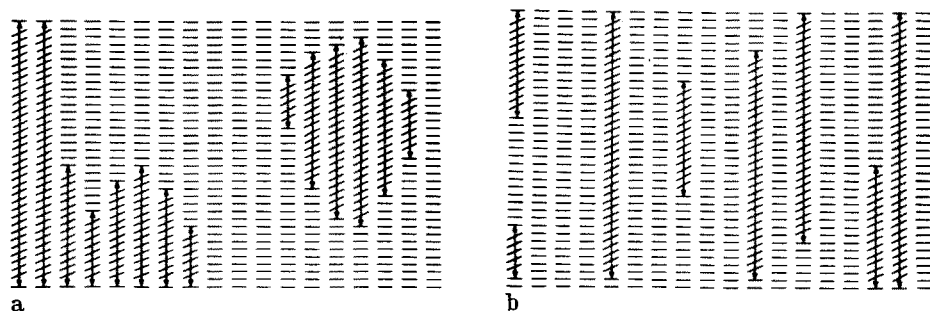


Fig. 3a and b. Heterogeneous (a) and homogeneous topochemical (b) reactions

the anisotropic lattice changes during the reaction^{15-25,31,32}. Most 2+2 cyclo-additions of olefins belong to this type of topochemical reactions (Fig. 3).

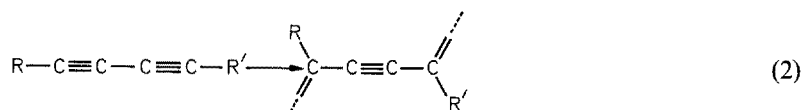
In the homogeneous reaction the product is randomly distributed in the parent crystal forming a solid solution. This mechanism leads in ideal cases to single crystal transformation although in some cases large changes of lattice parameters may be observed.

Homogeneous topochemical reactions are quite rare. The topochemical polymerization of diacetylenes and with special precautions some four center photodimerizations^{33,34} are examples for this reaction mode.

3 Structure and Reactivity

3.1 Packing of Diacetylene Monomers

The topochemical polymerization of diacetylenes proceeds by a 1,4-addition reaction according to:



The reaction is initiated by irradiation or by thermal annealing. The monomer units are arranged in a stack so that one monomer unit can react with its two neighbors. The polymer backbone which is formed in this process is oriented along a well defined lattice direction. A model of the monomer packing is schematically shown in Fig. 4. It can be characterized by the stacking distance d of the monomers in the array and by the angle Φ between the diacetylene rod and the stacking axis. In this model the

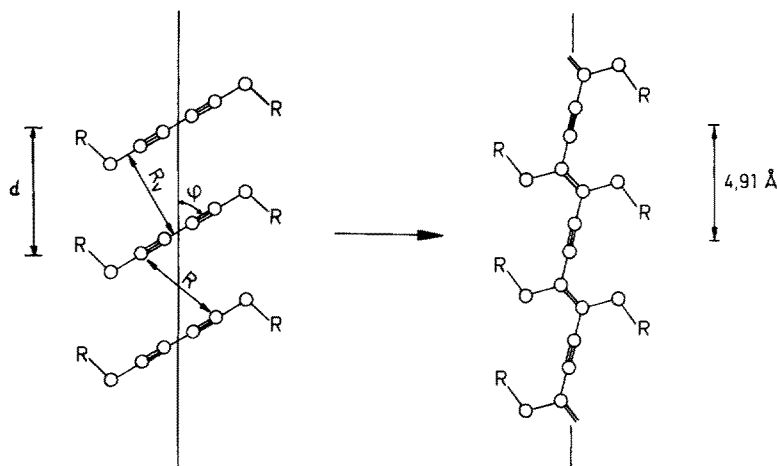
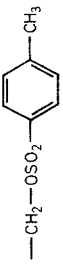
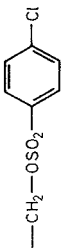
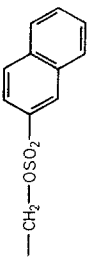
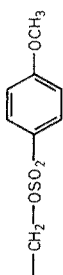
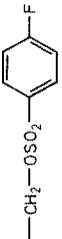
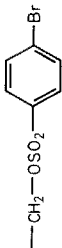
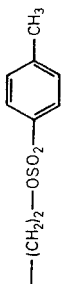


Fig. 4. Model for the packing of diacetylene monomers

Table 1. Packing parameters of diacetylene monomers $R-C\equiv C-C\equiv C-R'$

R	R'	Abbr.	Space group	Point group	d/Å	$\Phi/^\circ$	T/K*	Reactivity		Remark	Ref.
								Therm.	Gamma		
	= R	PTS	$P2_1/c$	$\bar{1}$	5.11	44	110	+++	+++	A	34-36)
	= R	PCS	$P\bar{1}$	$\bar{1}$	5.03	67	295	—	—		37)
	= R	PFBS	$P2_1/c$	$\bar{1}$	5.07	44.8	110	++	++		38)
	= R	PBS	$P\bar{1}$	$\bar{1}$	5.03	65.6	295	—	—		65)
	= R	MBS	$P\bar{1}$	$\bar{1}$	5.80	62.7	295	—	—		39)
	= R	NS	$P2_1/n$	$\bar{1}$	5.42	61.3	295	—	—		40)
	= R		$P\bar{1}$	$\bar{1}$	9.69	66.7	295	—	—		41)

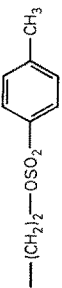
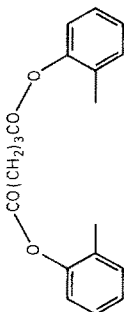
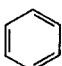
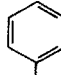
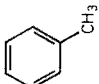
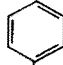
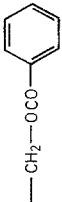
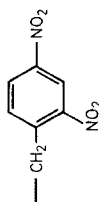

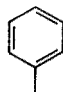
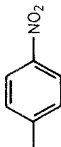
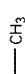
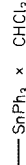

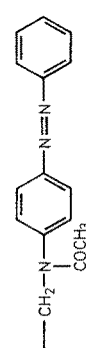
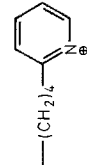

	= R	PTS-12	P1	1	5.19	47.9	110	—	—	B	42)
	cycl.	BPG-1	C2/c	2	4.93	46	110	—	+	C	43-45)
—Cz	= R	BPG-2	P21/n	1	5.42	90	295	—	—	—	46)
—CH2—Cz	= R	DCH	P21/c	1	4.66	90	295	—	—	—	47)
—CH2—A	= R	DAH	P21/c	1	4.55	60	295	+	+	B	48)
—CH2—Cz	—CH2A	ACH	P21/c	1	4.35	61.5	295	—	—	—	48)
—CH2—OCONH— 	= R	HDU-2	C2/c	1	4.00	66.7	110	(+)	(+)	E	31, 49, 50)
—(CH2)4—OCONH— 	= R	TCDU-1	P21/a	1	5.23	42.3	110	—	+	+	51)
—CH2—OCONH— 	= R	TCDU-2	P21/c	1	5.19	42.2	110	—	+	F	50)
—CH2OH	= R		C2/c	1	4.63	58.3	295	(+)	(+)	E	52)
CH2—CH2OH	= R		P21/c	1	4.76	41	295	(+)	(+)	—	53)
—CH2OH	—CH3		P21/c	1	4.85	45.5	120	—	+	—	54)
—CH2—O— 	= R		P21/c	1	4.87	49.6	110	—	+	G	55)
			Pcab	1	8.53	77	295	—	—	—	56)
			P21/c	1	4.35	73	295	—	—	—	

Table 1 (continued)

R	R'	Abbr.	Space group	Point group	d/Å	Φ/°	T/K*	Reactivity		Remark	Ref.
								Therm.	Gamma		
	= R		P2 ₁ /c	$\bar{1}$	4.35	58	295	(+)	—	H	57)
	= R	DNP	P2 ₁ /c	$\bar{1}$	8.48	40	295	—	—		
	= R		P2 ₁ /n	$\bar{1}$	5.19	45.7	295	++	+		58)
	= R		P2 ₁ /c	$\bar{1}$	6.04	51	295	—	—		59)
	= R		I4 ₁ /amd	mm	7.09	90	295	—	—		60)
	—C≡C—CH ₃		R3m	3/m	3.8	90	295	—	—		61)
	= R		Pa3	3	15.55	54.7	238	—	—		62)
	= R		Pa3	3	15.40	54.7	238	—	—		
	= R		P2 ₁ /c	$\bar{1}$	10.79	23.4	295	—	—		63)
	= R	TCNQ ^{•-}	P1	$\bar{1}$	6.94	47.8	295	—	—		64)

$-(CH_2)_3-OCONH-CH_2-COO-(CH_2)_3-CH_3$ = R	3BCMU	C2/c	$\bar{1}$	4.90	47.3	110	—	+	+	F	66)
$-(CH_2-OCONH-$  $-Cl)$ = R	P $\bar{1}$	P $\bar{1}$	$\bar{1}$	4.79	58.5	163	—	—	—	H	68)
$-C\equiv C-Si(CH_3)_3$ = R	Pbcn	Pbcn	1	—	—	295	—	—	—	I	69)
$-(CH_2)_3-OCONH-CH_2-COO-(CH_2)_3-CH_3$ = R	P $\bar{1}$	P $\bar{1}$	$\bar{1}$	4.94 4.03 4.45	83.5 65 59.5	295	—	—	—	J	67)
$-COOH \times H_2O$ = R	12/c	12/c	2	5.58	45	295	+	+	+		4)

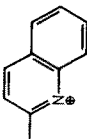
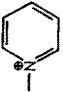
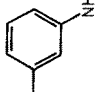
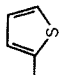
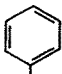

* Temperature at which the data collection for the structure analysis was carried out.

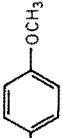
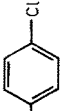
- A two independent molecules in the unit cell;
 B phase transition during the polymerization;
 C incomplete reaction;
 D order-disorder structure;
 E phase separation at a conversion of approximately 10 percent;
 F limiting conversion about 60 percent;
 G phase separation, residual monomer can be removed by sublimation;
 H low reactivity under pressure;
 I no stack structure;
 J three different intermolecular contacts in the unit cell;

—Cz: carbazolygroup;

—A: anthrylgroup

Table 2. Lattice parameters of diacetylene monomers $R-C\equiv C-C\equiv C-R'$. E.s.d.'s are given in parentheses

R	R'	Space group	a/Å	b/Å	c/Å	$\alpha/^\circ$	$\beta/^\circ$	$\gamma/^\circ$	Reactivity		Ref.
									Therm.	Gamma	
$-\text{CH}_2-\text{Cz}$	$-\text{CH}_2\text{OH}$	$P2_1/c$	18.22(4)	4.59(1)	16.99(4)		99.0(3)		—	—	⁷⁰⁾
$-\text{CH}_2-\text{N}(\text{Ph})_2$	= R	$P\bar{1}$	8.86(1)	10.08(1)	14.72(1)	110.7(1)	111.2(1)	81.7(1)	+++	+++	⁷¹⁾
$-\text{CH}_2-\text{N}(\text{Ph})_2$	$-\text{CH}_2-\text{Cz}$	$P2_1$	9.1	29.5	8.8		107.8		—	—	⁷⁰⁾
$-\text{CH}_2-\text{CH}_2-\text{N}^+\text{Cz}^-\text{TCNQ}^{2-}$ 	= R	$C222_1$	6.58(2)	19.50(3)	31.10(4)				—	—	⁷⁰⁾
$-\text{CH}_2-\text{CH}_2-\text{N}^+\text{Cz}^-\text{TCNQ}^{2-}$ 	= R	$P\bar{1}$	7.76(2)	13.87(2)	11.33(2)	93.1(3)	106.8(3)	102.4(3)	—	—	⁷⁰⁾
 $-\text{NH}-\text{CO}-\text{CH}_3$	= R	$P\bar{1}$	4.71(1)	16.10(3)	5.24(1)	93.7(5)	95.0(5)	77.0(5)	—	+	⁷⁰⁾
$-(\text{CH}_2)_4-\text{OCONH}-$ 	= R	$P2_1/c$	17.52(4)	6.52(3)	9.86(2)		97.0(3)		—	—	⁷²⁾
$-(\text{CH}_2)_4-\text{OCONH}-\text{CH}(\text{CH}_3)-$ 	= R	P1	9.83(3)	13.00(3)	12.43(3)	92.3(3)	91.6(3)	73.0(3)	—	(+)	⁷²⁾
$-(\text{CH}_2)_4-\text{OCONH}-$ 	= R	$P2_1/c$	16.87(2)	9.14(2)	9.55(2)		90.5(3)		—	—	⁷²⁾
$-(\text{CH}_2)_4-\text{Cz}$	= R	$C2/c$	19.28(1)	13.14(1)	10.92(1)		96.2(3)		—	(+)	⁷¹⁾

$-(CH_2)_L-OSO_2-$ 	R	$P\bar{I}$	5.24(2)	5.92(1)	21.29(2)	85.4(3)	96.6(3)	91.1(3)	—	(+)	⁷³⁾
$-(CH_2)_L-OSO_2-$ 	R	$P2_1/c$	21.19(2)	5.18(1)	11.53(3)		92.5(3)		—	(+)	⁷³⁾
$-(CH_2)_8-CH_3$	$-(CH_2)_8COOH$	$P\bar{I}$	4.76(4)	5.42(4)	42.3(8)	90	90	95.2(2)	—	+	^{74, 75)}
$-(CH_2)_{11}-CH_3$	$-COOH$	$P\bar{I}$	4.91(4)	5.36(5)	32.7(1)	90.5(2)	91.6(10)	106.7(10)	—	+	^{74, 75)}
$-(CH_2)_{11}-CH_3$	$-COOH$ × Phenazine	$P\bar{I}$	4.77(4)	7.09(5)	33.2(1)	91.5(2)	91.6(10)	104.5(10)	—	+	^{74, 75)}
$-(CH_2)_{13}-CH_3$	$-COOH$ × Phenazine	$P\bar{I}$	4.74(4)	7.15(5)	36.4(1)	84.1(2)	92.1(10)	106.1(10)	—	+	^{74, 75)}
$-(CH_2)_2CONHCH_2CH_3$	R	$P2_1/a$	16.82(10)	17.72(10)	4.70(1)			96.6(6)	+	+	⁷³⁾
CH_2OH	$-C\equiv C-CH_2OH$	$P2_1/c$	4.11	19.59	4.80		109	105(2)	—	—	⁷⁶⁾
$-C\equiv C-CH_2OCONH-Ph$	$-CH_2OCONH-Ph$	$P2_1/c$	24.65	30.74	4.89		92.2		(+)	+	⁷⁷⁾

approach of neighboring units is restricted by the van der Waals distance R_v . The polymer chain repeat distance of 4.91 Å as well as the bond lengths and angles of the polymer backbone are nearly constant for all cases studied to date (cf. Table 4). It should be emphasized at this point that there is normally a mismatch between the monomer stacking d and the polymer repeat. The consequences of the mismatch on the reaction kinetics will be discussed later.

In order to assess the relative reactivity of different diacetylene monomers the packing parameters can be analysed in terms of a reaction along a least motion reaction path, i.e. the molecules simultaneously rotate and translate along the stacking direction^{22, 23}. In this model maximal reactivity is expected for $d \simeq 5$ Å and $\Phi \simeq 45^\circ$. In Fig. 5 the values of the packing parameters d and Φ are plotted for constant separations R between the reacting atoms C1 and C4'. The relevance of the model considerations can be tested using crystal structure data, which have become available recently for a number of reactive and unreactive diacetylene monomers. Reactivity is only observed in a small area of the map. The distribution of the points for highly reactive structures suggest the criterion for which the separation R should be less than 4 Å to be a more critical condition than the requirement of a least motion pathway as calculated by Baughman^{17, 22, 23}. Figure 5 shows that all but one reactive diacetylene structure fulfill the 4 Å criterion. The exception DCH (cf. Table 1) is a special case where the reaction is connected with a phase transition. This will be discussed in detail later.

The dependence of the solid-state reactivity of diacetylenes on the packing parameters d and Φ are summarized in Table 1.

Crystallographic data of some monomers where the full crystal structure analysis has not been carried out are given in Table 2.

The experimental data qualitatively confirm the geometrical model presented in Fig. 4. The reactivity is controlled by the monomer packing and not by the chemical nature of the substituents. In many cases different modifications of a specific monomer can be obtained which exhibit drastic differences in reactivity³¹. However, it should be emphasized at this point that the packing parameters give no absolute scale for

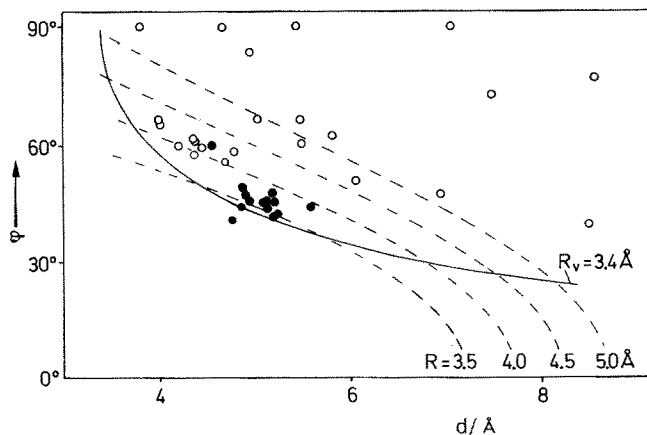


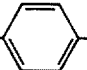
Fig. 5. Plot of d vs. Φ . The broken lines are lines of constant distance R between C1 and C4'. ○: inactive structures, ●: reactive structures

the reaction rate. Monomers with virtually identical packing can show large reactivity differences. Some cases will be discussed in detail below.

3.2 Crystal Structure Analysis of Diacetylene Monomers

Until 1977 no crystal structure analyses were known for highly reactive diacetylene monomers. Polymerization in the primary x-ray beam proceeds in these cases so rapidly that data collection on the monomer crystal is impossible. This experimental difficulty was overcome by carrying out the data collection at low temperatures. At 110 K the polymerization rate is sufficiently low to maintain a polymer content at below 5 percent during the time necessary to collect the data for an average structure.

The first monomer crystal structure which was solved using this technique was PTS

($R = R' = -CH_2OSO_2-$  $-CH_3$, cf. Table 1) which is regarded in many respects as

a model for the whole class of diacetylenes^{34, 35}). A projection of the monomer and polymer crystal structures on a common plane is shown in Fig. 6^{78, 79}).

Stereoscopic views of the packing in both structures are shown in Fig. 7.

The experimental result is in agreement with the simple geometrical model presented in Fig. 4. The packing parameters are in the range where high reactivity is expected. In a first approximation the side group packing can be considered to remain unchanged and all molecular motions are restricted to the center of the molecule. This is necessary for the formation of a solid solution of growing polymer chains in the monomer matrix. The crystallographic data given in Table 3 show that monomer and polymer crystal structures are indeed isomorphous although considerable lattice changes are involved in the reaction. These will be analysed in detail below.

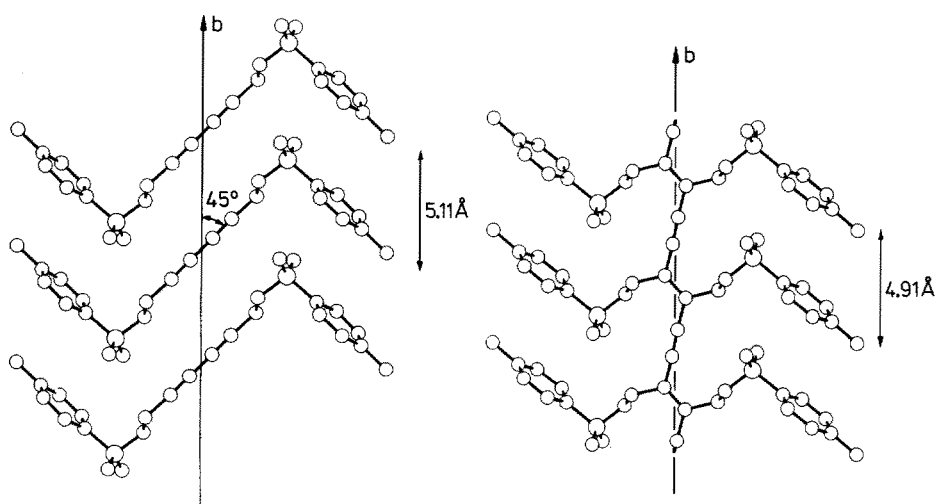


Fig. 6. Projection of the PTS monomer and polymer crystal structures on the plane of the polymer backbone

Table 3. Lattice parameters of crystal structures as discussed in detail in the text. E.s.d.'s are given in parentheses

Structure	T/K	a/Å	b/Å	c/Å	$\alpha_i/^\circ$	$\beta/^\circ$	$\gamma/^\circ$	D _x g/cm ³	Space group	Ref.
PTS monomer	120	14.61(1)	5.11(1)	25.56(2)		92.0(5)		1.46	P2 ₁ /c	34, 35)
PTS monomer	295	14.60	5.15	15.02		118.4		1.40	P2 ₁ /c	80)
PTS monomer	295	14.65(1)	5.178(2)	14.94(1)		118.81(3)		1.40	P2 ₁ /c	81)
PTS polymer	295	14.993(8)	4.910(3)	14.936(10)		118.14(4)		1.483	P2 ₁ /c	78)
PTS polymer	120	14.77(1)	4.91(1)	25.34(2)		92.0(5)		1.51	P2 ₁ /c	79)
TCDU-1 monomer	120	7.08(2)	33.97(3)	5.23(2)		115.8(5)		1.26	P2 ₁ /a	51)
TCDU-1 polymer	295	6.229(5)	39.027(1)	4.909(4)		106.85(5)		1.25	P2 ₁ /a	83)
TCDU-2 monomer	120	18.97(4)	5.19(2)	11.60(2)		92.0(5)		1.26	P2 ₁ /c	50)
TCDU-2 50 Mrad	295	19.65(4)	4.96(2)	12.12(3)		92.5(5)		1.23	P2 ₁ /c	50)
TCDU-2 65 % pol.	295	19.63(1)	4.95(1)	11.84(1)		94.9(1)		1.25	P2 ₁ /c	50, 82)
DCH monomer	295	13.60(5)	4.55(2)	17.60(5)		94.0(5)		1.25	P2 ₁ /c	47)
DCH monomer	110	13.38(1)	4.20(4)	18.44(1)		92.0(5)		1.31	P2 ₁ /c	48)
DCH polymer	295	12.87(1)	4.91(1)	17.40(1)		108.0(2)		1.30	P2 ₁ /c	84)
DCH polymer	295	12.821(4)	4.886(3)	17.328(3)		108.32(3)		1.31	P2 ₁ /c	70, 85)
PTS-12 monomer	110	20.60(2)	11.79(1)	5.19(1)	83.0(3)	89.2(3)	92.7(3)	1.36	P $\bar{1}$	42)
PTS-12 polymer	110	20.01(2)	6.02(1)	4.91(1)	95.1(3)	93.7(3)	88.7(3)	1.42	P $\bar{1}$	42, 85)
PTS-12 polymer	295	20.13(2)	6.11(1)	4.91(1)	95.1(3)	93.7(3)	88.7(3)	1.39	P $\bar{1}$	42)

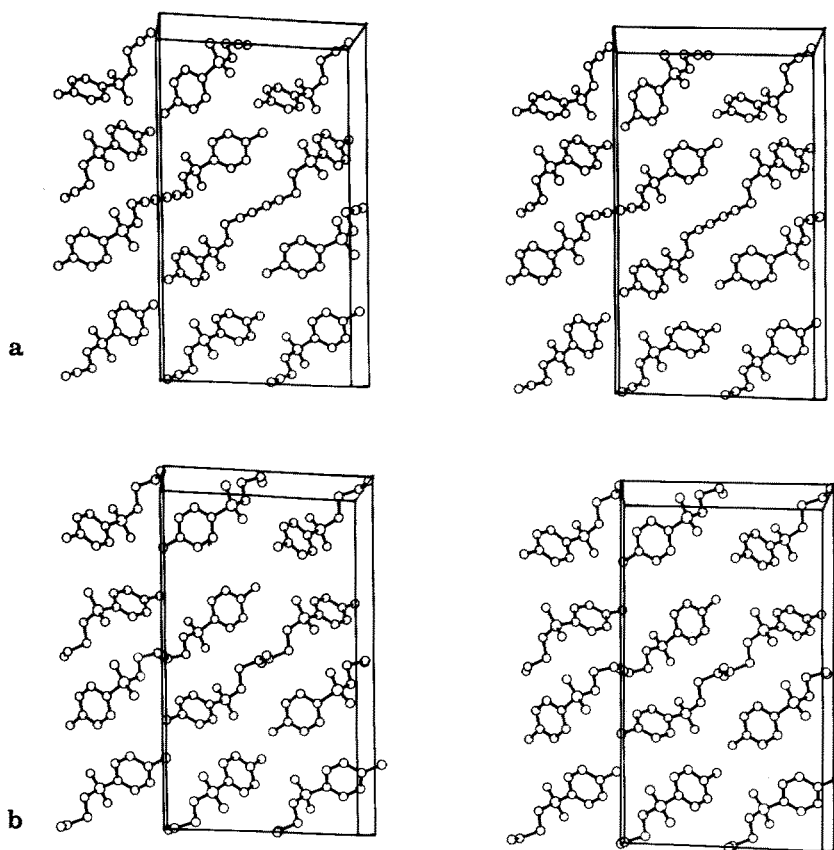


Fig. 7a and b. Stereoscopic projections of the packing of PTS monomer (above) and polymer (below) at 120 K. **a** is horizontal and **b** vertical

3.3 Molecular Motions Connected with the Topochemical Polymerization of Diacetylenes

The simple geometrical model of the least motion principle neglects the contributions of the side group packing, which is thought to remain constant during the reaction. PTS is in many respects a model compound where this ideal condition is nearly satisfied. In many other cases, however, side group packing and mobility play a dominant role in polymerization. The cyclic monomer BPG is an example where the reactivity is restricted by the side group packing. Despite of favourable monomer packing ($d = 4.93 \text{ \AA}$, $\Phi = 46^\circ$, Fig. 8) BPG cannot be polymerized quantitatively. At a gamma-ray dosage of 60 Mrad a limiting conversion of approximately 35 percent is reached^{43,44}). This unexpectedly, low reactivity can be qualitatively understood by the fact that the large cyclic side group is directly attached to the reactive triple bond system. This restricts the side group mobility which is necessary in addition to favourable monomer packing. Tables 1 and 2 show that in order to attain high reactivity the diacetylene group and the side group must be separated by at least a

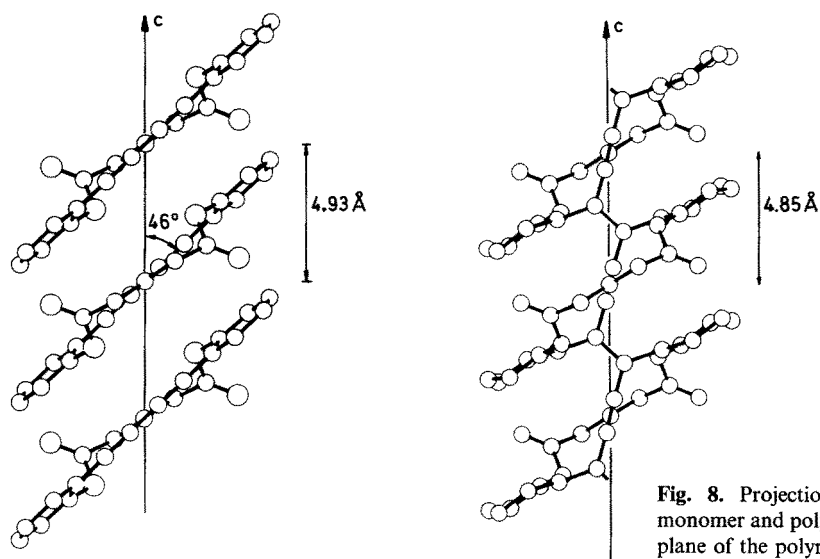
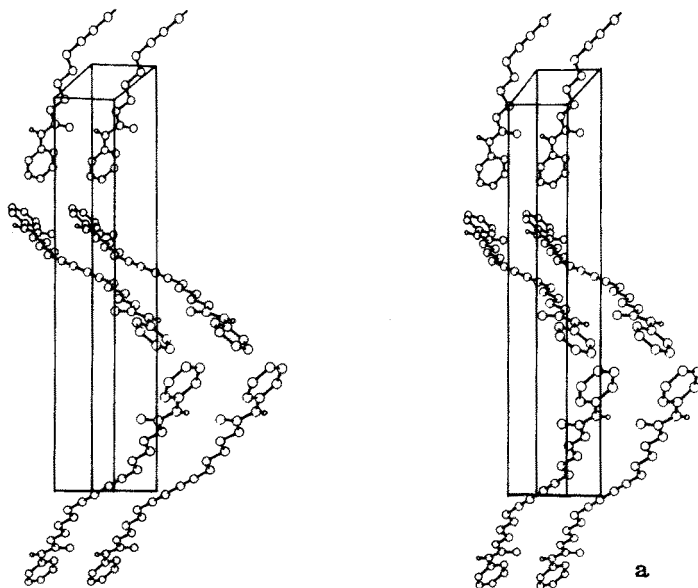


Fig. 8. Projection of BPG monomer and polymer on the plane of the polymer chain

methylene group acting as a mobile spacer. This empirical rule holds with very few exceptions.

Even if this condition is fulfilled the reactivity can be restricted by the mutual sidegroup motions. TCDU and 3BCMU (cf. Table 1) are examples for this behaviour. TCDU can be obtained in two different modifications in which monomer stacks with almost identical packing parameters are packed together in different ways^{50, 51}. Stereoscopic projections of the crystal structures are shown in Fig. 9, pertinent crystallographic data are summarized in Table 3.



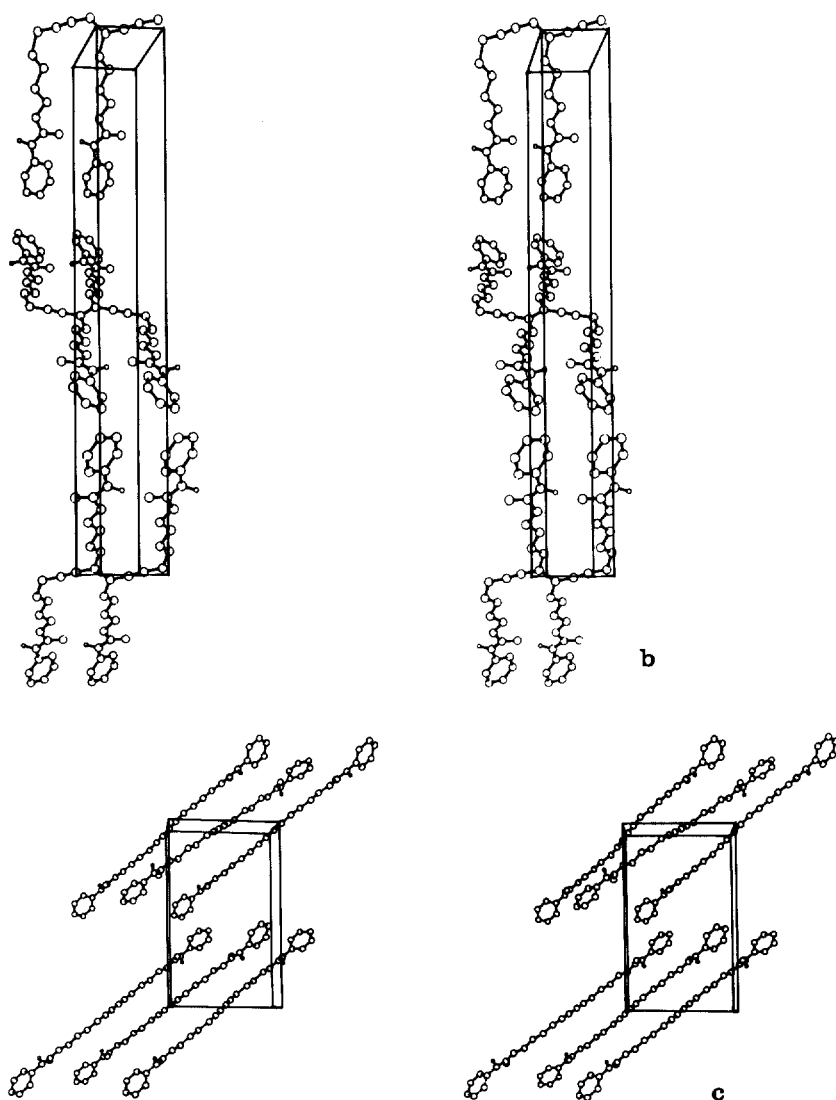


Fig. 9a-c. Stereoscopic projections of the packing in TCDU structures. a) TCDU-1 monomer, b) TCDU-1 polymer, b is vertical and c horizontal. c) TCDU-2 monomer, a is vertical and c horizontal

TCDU-1 can be polymerized with ^{60}Co γ radiation to an almost complete conversion. However, the reaction is accompanied by unusually large rotations of the entire side chain which is evidenced by the large change of the b axis (13 %, Table 3) in going from monomer to polymer. This introduces some disorder which can be detected in unusual bond lengths in the polymer structure and large thermal parameters ⁸³.

Although TCDU-1 and TCDU-2 have very similar packing parameters TCDU-2 is much less reactive, e.g. at a dosage of 50 Mrad the stacking axis b is decreased to 4.95 Å. From this value a conversion of about 60 percent can be calculated using the known conversion dependence of the stacking distance in other reactive diacetylenes.

At this point the crystals already have suffered from radiation damage or other disorder introduced by the reaction. Higher order reflections, especially those with $l > 3$ begin to vanish indicating some disorder along the c-axis which roughly corresponds to the orientation of the side chain. Attempts to solve the crystal structure of the polymer with the limited available data have failed⁸²⁾. The differences in the reactivity of both modifications can be qualitatively explained by the mutual side group motions. In TCDU-2 neighboring monomer arrays are related along the c-axis by a glide plane. As a consequence of this "antiparallel" orientation, alternating sheets of molecules perform movements in opposite directions which may be the cause for the limited reactivity and the disorder introduced during the reaction. Similar observations have been made with 3BCMU⁶⁶⁾.

4 Polymer Growth in the Monomer Matrix

4.1 Structural Investigations

PTS can be regarded in many respects as a model for the whole class of diacetylenes. The monomer can be easily prepared and obtained as large and perfect single crystals. Thermal polymerization occurs even at room temperature so that the reaction can be carried out under very mild conditions^{80,86)}. Time conversion curves for three different polymerization temperatures are shown in Fig. 10. The polymerization is characterized by a slow induction period followed by a rapid reaction to complete conversion. Both reaction regimes show apparent first order kinetics with identical thermal activation energies of 92 kJ/mol⁸⁷⁻⁹⁰⁾.

The conversion dependence of the lattice parameters of PTS is plotted in Fig. 11. Over the entire conversion range the lattice parameters change gradually from their initial to their final values³⁵⁾. Although polymerization proceeds with quite large changes of some lattice parameters no phase separation is observed and the high crystal quality is retained in all conversions. A wide range of experimental techniques

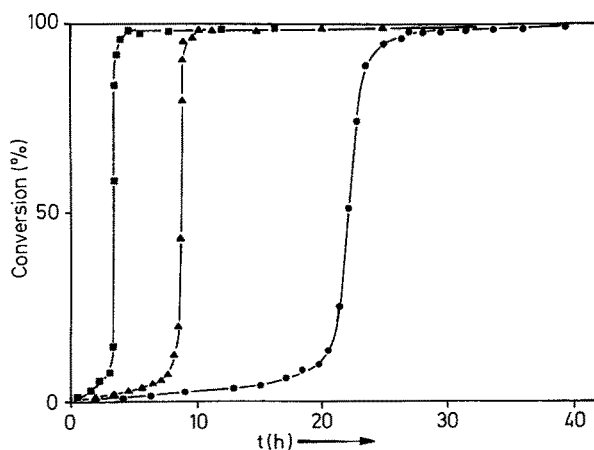


Fig. 10. Time conversion curves for the thermal polymerization of PTS. ●: 60 °C, ▲: 70 °C, ■: 80 °C

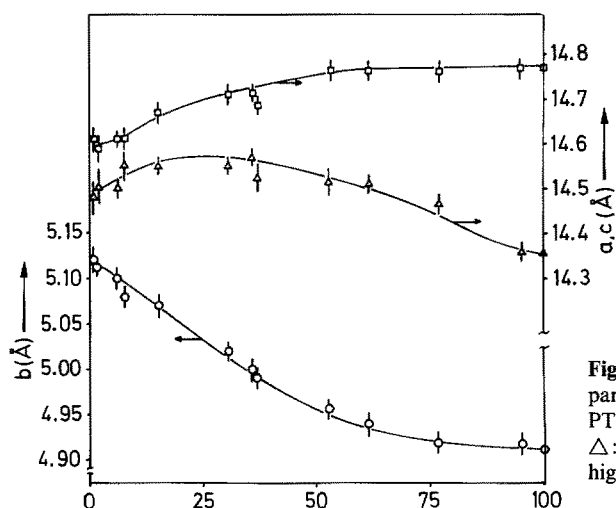


Fig. 11. Dependence of the lattice parameters determined at 110 K for PTS on the conversion. ○: *b*, □: *c*, △: *a*. The values plotted refer to the high temperature cell

have been used in studies of PTS polymerization. All experimental results indicate that the thermal polymerization of PTS is very close to the limiting case of an ideal homogeneous topochemical reaction. The randomly distributed polymer chains can be regarded as one-dimensional defects giving rise to diffuse sheets in x-ray and neutron scattering experiments which are oriented perpendicular to the chain direction⁹¹⁻⁹⁵. The width of the sheets can be used for a rough estimate of the average chain length as a function of conversion. In the initial stages of polymerization the intensity of diffuse scattering increases. At higher conversions the correlations between chains become increasingly important and are visible as intensity modulations, and finally the diffuse scattering vanishes when complete conversion is reached.

Similar results have been obtained by measuring the Raman spectra of partially polymerized crystals and by other spectroscopic techniques. Here, the vibrational frequency of the polymer chain can be used as a probe for the lattice strain in the vicinity of the dispersed macromolecules^{96,97}. It should be noted that monomer and polymer are not strictly isomorphous. The mismatch between monomer stacking and polymer repeat of 0.2 Å per addition step has to be accounted for by the monomer matrix. The raman frequencies shift accordingly to the lattice changes (cf. Fig. 11) in agreement with the random chain distribution.

A polymerizing diacetylene crystal can be considered as a composite material with large differences in the mechanical properties of both components. In such a material the mechanical properties will not only depend on the relative amount of the components but also very strongly on the geometrical arrangements of the structural elements⁹⁸⁻¹⁰⁰. Two limiting cases can be considered: The first model consists of infinite rods of the high modulus material (polymer chain) embedded randomly in the soft monomer matrix and aligned in direction of the strain. This model of a reinforced material has been treated by Voigt⁹⁸. Here, the elastic constant *c* depends linearly on the volume fraction *v_p* of the polymer according to:

$$c = (1 - v_p) c_m + v_p c_p \quad (3)$$

c_m and *c_p* being the elastic constants of the monomer and polymer, respectively.

The other limiting case (Reuss model) of a two component material is a sandwich structure of alternating layers of high and low modulus materials loaded perpendicular to the layer plane⁹⁹⁾. In this case the stress is uniformly distributed within the sample. The resulting modulus is given by:

$$\frac{1}{c} = \frac{1 - v_p}{c_m} + \frac{v_p}{c_p} \quad (4)$$

The two theoretical curves are plotted in Fig. 12 as a function of conversion together with the experimental values of the elastic constant c_{22} of PTS in chain direction which have been obtained by Brillouin scattering^{35,101)}. At higher conversions the experimental data are very well represented by the Voigt model. The deviation at low conversions can be explained by the limited length of the polymer chains and have been used to assess the average degree of polymerization.

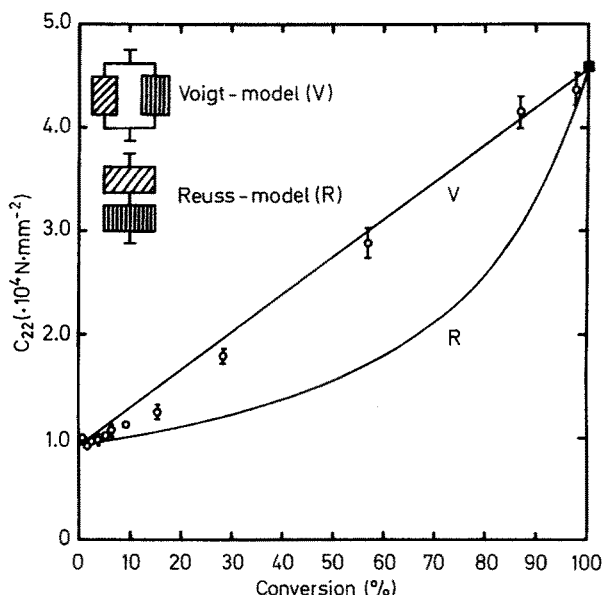


Fig. 12. Dependence of the elastic constant c_{22} in chain direction on the conversion in partly polymerized PTS crystals. The black square is the theoretically expected value for the pure polymer. The curves marked (V) and (R) are calculated according to Eq. (3) and (4), respectively

4.2 The Crystal Strain Theory

A theory of the polymerization kinetics of diacetylenes has been developed by Baughman¹⁰²⁾ on the basis of these findings, i.e. that the polymer is formed in the monomer lattice which it does not match. The resulting strain plays a crucial role in the theory. The following assumptions have been made:

- 1) In all conversion monomer and polymer units form a solid solution. The separation d in chain direction between lattice sites is conversion dependent.
- 2) Initiation is constant and conversion dependent.
- 3) The propagation rate is given by the product of the conversion independent life

time τ of the active chain end and the conversion dependent kinetic chain length L_n :

$$k_p = L_n \tau \quad (5)$$

- 4) The conversion dependence of L_n can be split into two parts. First, the probability of termination by a previously formed chain in the same stack or lattice defects will increase with conversion. Secondly, the activation energy for the addition of one monomer unit can be approximated by:

$$E_a(X) = D(d(X) - d_p)^2 \quad (6)$$

where D is the force constant in stacking direction and $d(X)$ and d_p the stacking distances at a conversion X and in the pure polymer, respectively.

In a system described by a Voigt model (refer to Eq. 3) Eq. (6) can be rewritten as:

$$E_a(X) = (d_m - d_p)^2 c_m \left[\left(1 + \frac{X}{1-X} \left(\frac{c_p}{c_m} \right)^{-2} - 1 \right) \right] \quad (7)$$

The theory was used to calculate kinetic curves for the polymerization of PTS deducing the ratio c_m/c_p from the known conversion dependence of the lattice parameters. Time conversion curves normalized with respect to the time necessary to reach 50 percent conversion can be calculated for different values of the lattice mismatch using the crystal strain theory. For PTS a satisfactory fit of the experimental data of the thermal and γ -ray polymerization can be obtained. However, further studies of the kinetics of the solid-state polymerization of PTS and other monomers provided results which cannot be explained by the theory.

First, the thermal polymerization of PTS is strongly affected by isotope substitution^{88,89}. Deuterated and partially deuterated samples show an unusually large inverse isotope effect, i.e. during the induction period the reaction rate is increased by a factor up to 3.5. In the rapid reaction regime, however, a small normal isotope effect, i.e. a small decrease of the polymerization rate is observed. The magnitude of the isotope effect is largest if the units adjacent to the diacetylene group are substituted. Even substitution of the methylene spacer group with ^{13}C has a marked effect on the kinetics. Lattice parameters and thermal activation energies are in all cases unaffected by the isotope substitution. Secondly, the induction period can be suppressed by moderate hydrostatic pressure so that the overall polymerization kinetics becomes nearly first order¹⁰³. The analysis of this effect shows that both the decrease of the induction period and acceleration of the rapid reaction are larger than predicted with the elastic strain theory using the known lattice parameters and elastic constants¹⁰⁴.

Finally, there is experimental evidence that the thermal polymerization of some monomers with mismatches comparable to PTS cannot be described by the elastic strain theory^{105,106}.

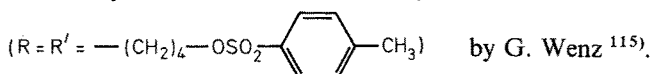
The polymerization kinetics of diacetylenes is discussed in detail elsewhere¹⁰⁷. Some of the failures of the theory may be due to the assumptions and approximations made in the calculations. Baughman and Chance have tried to explain some of the above mentioned effects by introducing a chain-terminating impurity¹⁰⁸. The concentration of this impurity, however, cannot be independently determined and must be fitted according to the experimental results.

4.3 Reaction Kinetics and Molecular Weight Distribution

One of the shortcomings of the elastic strain theory which leaves room for further improvements is the fact that assumptions must be made about the individual initiation, propagation and termination steps which cannot be observed independently but are calculated from the overall reaction rate.

A deeper insight into the reaction mechanism may elucidate the conversion dependence of the molecular weight and its distribution. Owing to the extreme insolubility of the better investigated polydiacetylenes like PTS, however, only very limited experimental data have been available until recently from indirect determinations, e.g. from mechanical properties or diffuse scattering of partially polymerized crystals.

Since Patel discovered in 1978 that poly3BCMU ($R = R' = -(\text{CH}_2)_3-\text{OCONH}-\text{CH}_2-\text{COO}-(\text{CH}_2)_3\text{CH}_3$, cf. Table 1) is a readily soluble polymer the study of the solution properties of polydiacetylenes attracted increasing interest^{66,109-115}. With such samples the molecular weight and its distribution can be determined using standard techniques and related to the conversion and other experimental parameters. This analysis has been carried out in great detail for PTS-12



The dosage conversion curve for the polymerization of PTS-12 by ^{60}Co radiation is plotted in Fig. 13 for two temperatures. It is characterized by an induction period followed by a rapid reaction leading to complete conversion which is reached at about 15 Mrad. The onset of the rapid reaction is connected with a phase transition which will be discussed later.

The development of the molecular weight distribution with increasing conversion as determined by gel permeation chromatography is shown in Fig. 14. During the

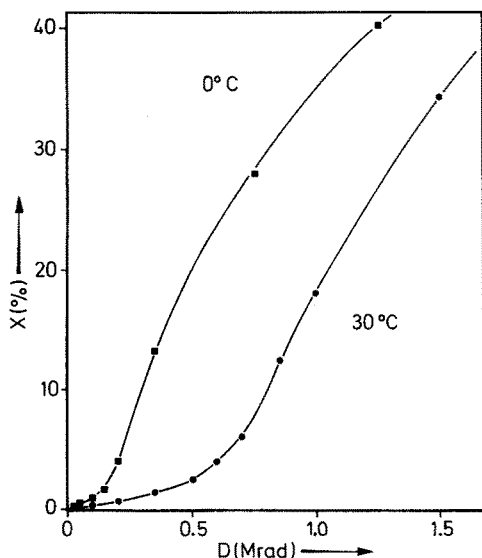


Fig. 13. Dosage conversion curves for the polymerization of PTS-12 at 0 °C and 30 °C

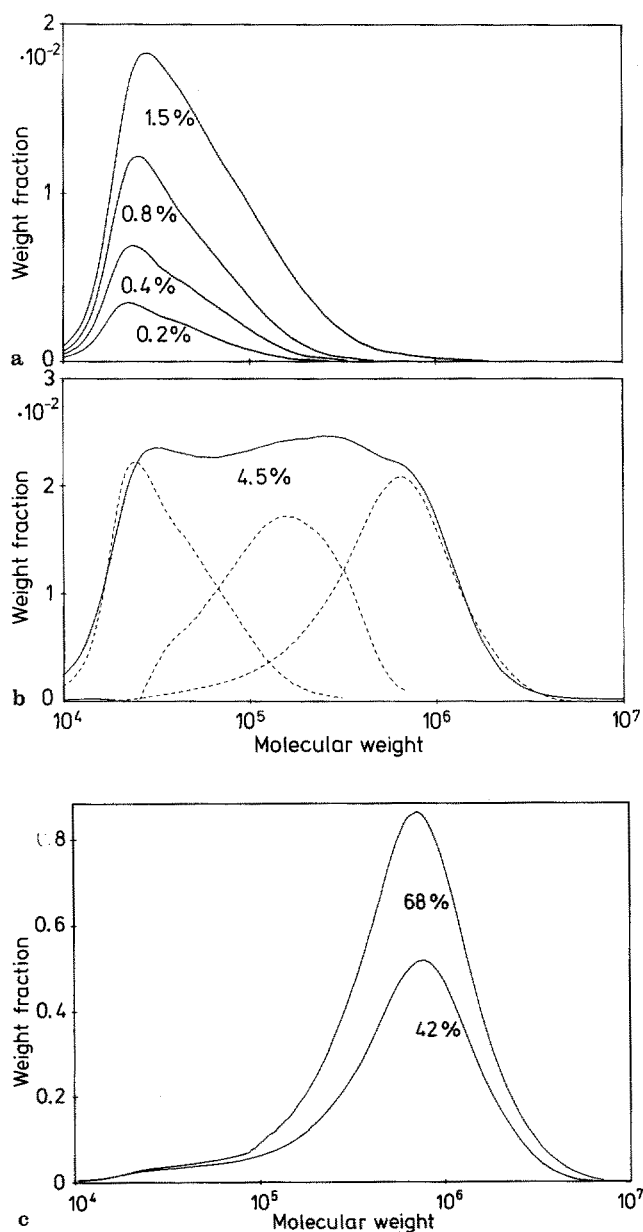


Fig. 14a-c. Molecular weight distribution of PTS-12 at three different stages of polymerization. a) initial stage, b) intermediate stage, c) final stage

induction period short chains with an average degree of polymerization $P_n = 60$ are formed. At higher conversions the maximum rapidly shifts to higher values. Three distribution curves with maxima at $P_n = 60$, 200 and 800 can be fitted to the experimental chromatograms. This is evident for the intermediate conversion range. Above approximately 20 percent conversion only the high molecular weight product is formed.

Analysis of the kinetic data shows that the chain initiation rate is constant at $k_i = 6.25 \cdot 10^{-4} \text{ Mrad}^{-1} [G = 1.2 (100 \text{ eV})^{-1}]$. Therefore, the sudden increase of the overall reaction rate in the rapid reaction regime must be attributed to an increase of the kinetic chain length.

It is interesting to note that the short chains formed initially remain intact. This means that there is no re-initiation of "dead" chain ends and no combination of an active chain with a dead polymer present in the same stack. Consequently, two different termination reactions must be considered. In the "free" termination an active chain end is deactivated by a limited life time or some unknown chemical reaction. At higher conversions, however, the "enforced" termination becomes increasingly important; a growing chain is blocked by an already existing polymer. In this kinetic scheme the kinetic chain length L is given by the ratio of the propagation and initiation rates. In Fig. 15 L is compared with the momentaneous degree of polymerization P_n which can be independently determined from difference distributions. Within the experimental error both L and P_n follow the same conversion dependence.

The propagation rate is strongly temperature dependent as already obvious from Fig. 13. In Fig. 16 molecular weight distributions after irradiation with 0.05 Mrad are compared at three different temperatures.

All distribution curves are bimodal with maxima at $P_n = 60$ and 400. At lower temperatures longer chains are formed. Since there is no gradual shift of the maximum with temperature it must be assumed that the chain grows by at least two different active chain ends, the population of which is strongly temperature dependent. The chemical nature of these chain ends cannot be deduced by the kinetic data. However, it seems reasonable to infer that we are dealing with the same carbene and radical intermediates which have been identified in the photopolymerization of diacetylenes at low temperatures by Sixl and coworkers¹¹⁶⁾.

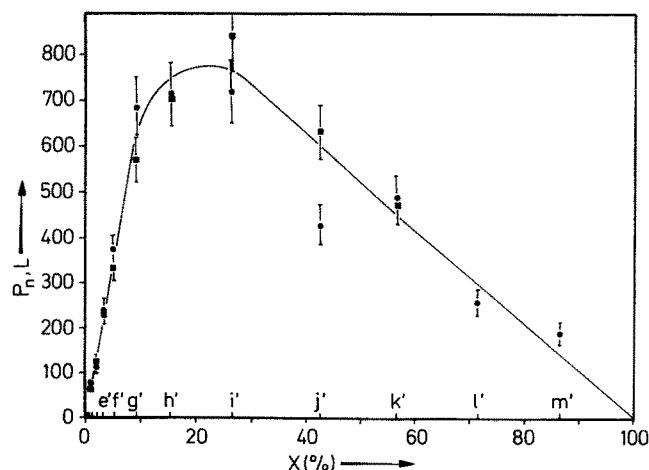


Fig. 15. Comparison of the conversion dependence of the kinetic chain length L (●) and the momentaneous degree of polymerization P_n (■) of PTS-12

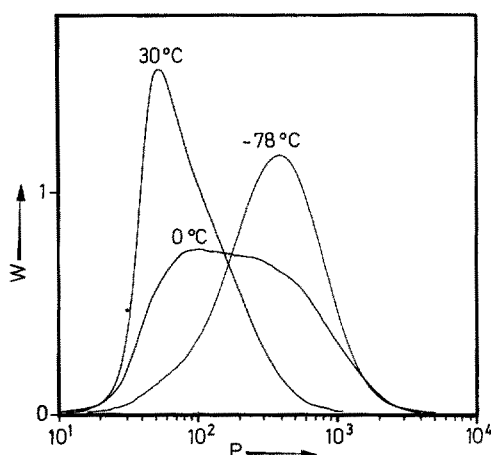
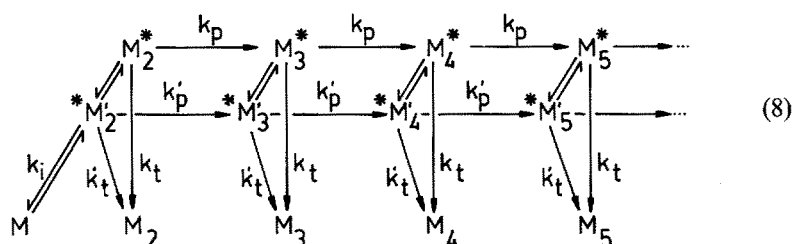


Fig. 16. Temperature dependence of the molecular weight distribution of PTS-12 after irradiation with 0.05 Mrad

The following reaction scheme for the polymerization of PTS-12 can be proposed:



It appears that the reaction mechanism and the intermediates involved in the solid-state polymerization of diacetylenes are reasonably well understood. However, experimental results obtained with special monomers should not be generalized. It is not possible to design a monomer with desired properties. Inspection of Table 1 shows that on the basis of the crystallographic data and the monomer packing the absolute reactivity and the polymerization kinetics cannot be quantitatively predicted, e.g. it is not possible, to date, to explain why certain diacetylenes can be polymerized thermally whereas others with equal packing are thermally inactive. A more realistic kinetic model should include the various energy transport processes and the complex side group motions which are connected to the reaction.

5 Phase Transitions

The gradual conversion of the monomer crystal into the equivalent polymer crystal can be considered a special type of phase transition. In some cases the topochemical polymerization is accompanied by an additional structural phase transition. This behaviour is most often observed in monomer structures with a comparatively moderate reactivity where only a partial conversion can be achieved. Here, the side group packing is rearranged either spontaneously or by thermal annealing. This process

usually leads to phase separation and nucleation of a new, more reactive monomer modification which is subsequently polymerized. The monomer crystal disintegrates in this type of transition although the deposition of the reactive monomer phase may be topotactic, i.e. oriented along certain crystallographic directions leading to a fibrous texture ^{26, 31, 49}).

In some special cases, however, both the polymerization and the side group reorientation are single phase processes. They are of special interest for understanding the dynamics and side group mobility in the solid-state polymerization of diacetylenes.

5.1 Conversion Dependent Phase Transition in DCH

1,6-Di-(N-Carbazolyl)-2,4-Hexadiyne (DCH) represents such a limiting case for the topochemical polymerization. The packing parameters, $d = 4.55 \text{ \AA}$ and $\Phi = 60^\circ$ are well outside the range where high reactivity is expected (cf. Fig. 5). Indeed, the polymerization of DCH in the x-ray beam proceeds so slowly that the data collection for the crystal structure analysis could be carried out at room temperature ⁴⁷).

The dosage conversion curve shown in Fig. 17 shows a distinct induction period. Analysis of the Brillouin scattering has demonstrated that in this range very short chains are formed ¹¹⁷).

At a conversion of approximately 25 percent the crystals undergo a phase transition which is evidenced by a sudden change of all lattice parameters (Fig. 18). Especially the monoclinic angle β abruptly changes by 14 degrees during the transition.

Pertinent crystallographic data are summarized in Table 3 and projections of the monomer and polymer structures are shown in Fig. 19 and Fig. 20.

Below the critical conversion the polymer forms a solid solution in the monomer phase. In this state the mismatch is exceptionally large and the polymer chains are contracted by 8 percent. After the transition the situation is reversed and the residual monomer occupies lattice sites within the polymer structure. Here, the packing is much more favourable for the polymerization, which proceeds with large speed.

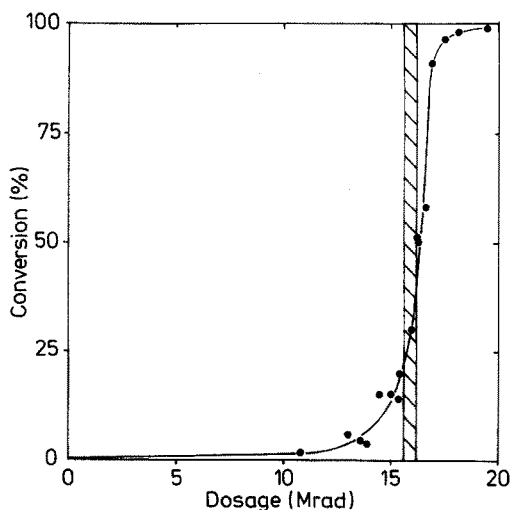


Fig. 17. Dosage conversion curve for the polymerization of DCH

In Fig. 18 it can be seen that the carbazole rings retain their stacking distance of 3.35 Å during the transition. This is only possible by a large rotation of the rings about the N-C3 bond. The large shearing of the lattice results from this side group reorientation. It should be emphasized that although we are dealing with a displacive phase transition it proceeds homogeneously throughout the crystal in γ -ray polymerization introducing only little disorder. During the transition the crystal shape changes according to the microscopic changes of unit cell dimensions, i.e. the crystals expand by 8 percent along b and are sheared according to the change of β .

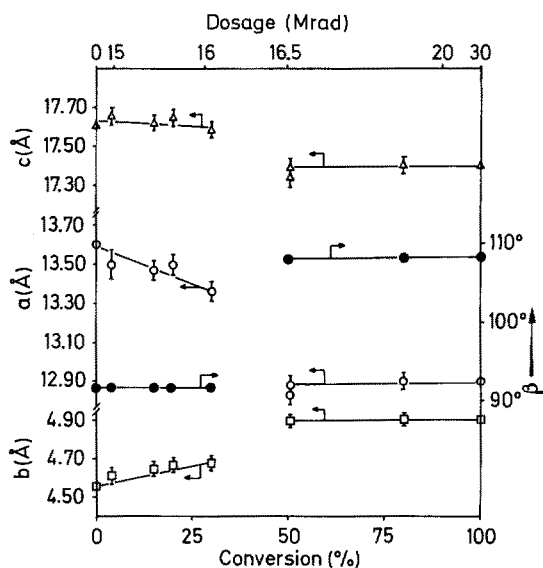


Fig. 18. Conversion dependence of the lattice parameters of DCH

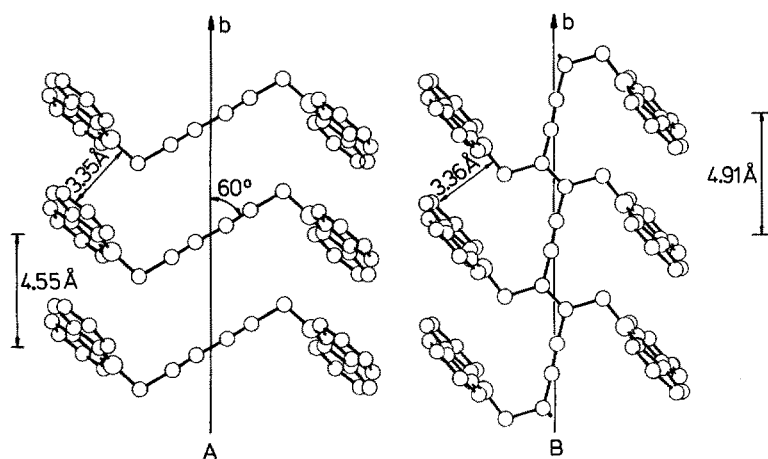


Fig. 19. Projection of the DCH monomer and polymer crystal structures on the plane of the polymer chain

It is interesting to note that in contrast to these results the thermal polymerization of DCH always proceeds heterogeneously with nucleation of separate polymer domains. The thermal polymer is polycrystalline with a fibrous texture. Lattice parameters are identical with those of the polymer obtained by irradiation. Observation of thermally polymerizing DCH crystals shows that the reaction starts at crystal

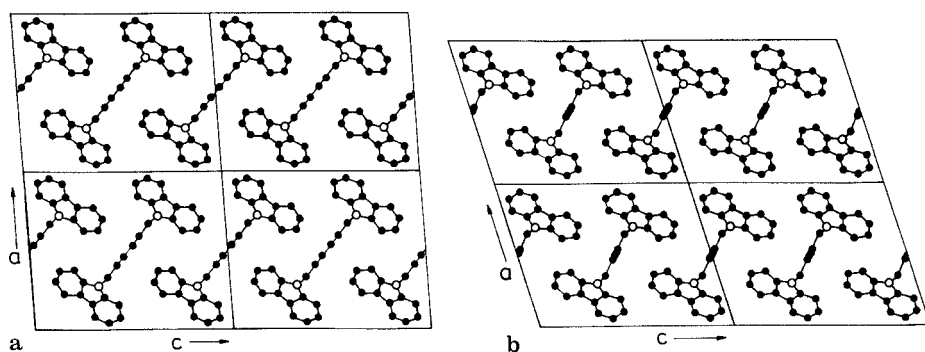


Fig. 20a and b. DCH monomer (a) and polymer (b) crystal structures

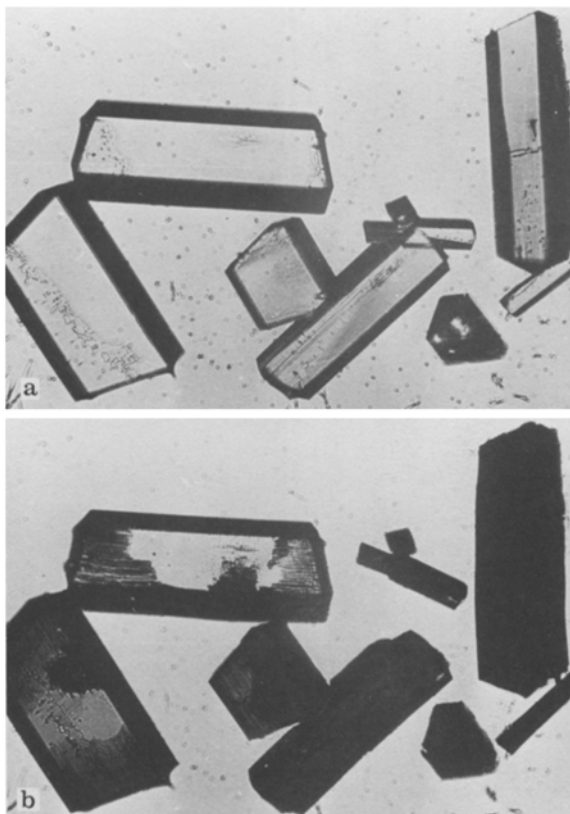


Fig. 21a and b. Thermal polymerization of DCH. a DCH monomer; b after 20 hours at 120 °C

edges or other visible defects. Phase separation then continues by growth of several separate daughter phases inside the monomer crystal. This eventually leads to the destruction of the monomer crystal.

In Fig. 21 DCH crystals are shown before polymerization and at an intermediate conversion. It is typical for the thermal reaction that more perfect monomer crystals require longer reaction times than defect-rich crystals. There is evidence that in the radiation polymerization of DCH the polymer crystal perfection increases with decreasing temperature, i.e., the nucleation process requires a rather high thermal activation energy.

5.2 Conversion Dependent Phase Transition in PTS-12

Another phase transition which casts an interesting light on the side group motions is observed during the polymerization of PTS-12⁴²⁾. The onset of the rapid reaction (cf. Fig. 13) is accompanied by this transition. In the monomer the *b* axis is doubled. The transition can be monitored by a continuous decrease of the intensities of all reflections having odd *k* indices. The dependence of lattice parameters on conversion is plotted in Fig. 22, pertinent crystallographic data are given in Table 3. The doubling of the monomer unit cell is explained by the fact that in contrast to the polymer chain the monomer unit is not centrosymmetric. Two differently oriented side chains are attached to the reactive triple bond system. This gives rise to a packing arrangement where the centers of the diacetylene groups in neighboring arrays are alternatingly

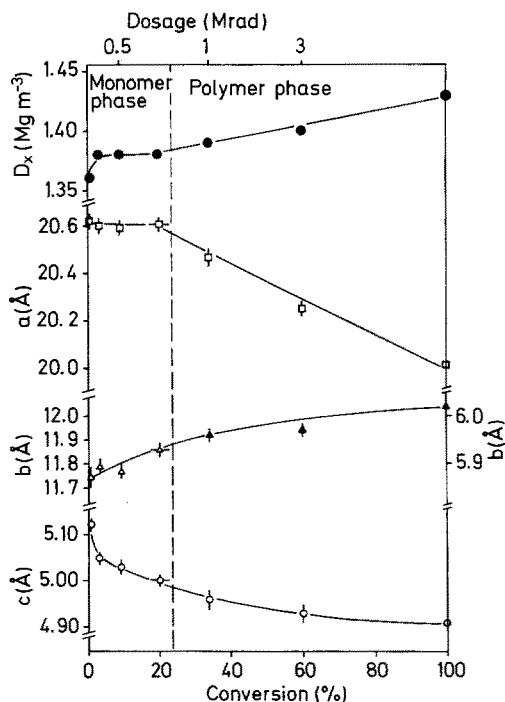


Fig. 22. Conversion dependence of the lattice parameters of PTS-12 determined at 110 K.

above and below the lattice site they assume in the polymer structure. This is quite surprising since in addition to the rotation of the diacetylene group a translation of approximately 1 Å is necessary for the reaction which proceeds without phase separation or macroscopic deformation of the crystal.

A projection of the monomer and polymer crystal structures onto a common plane is shown in Fig. 23.

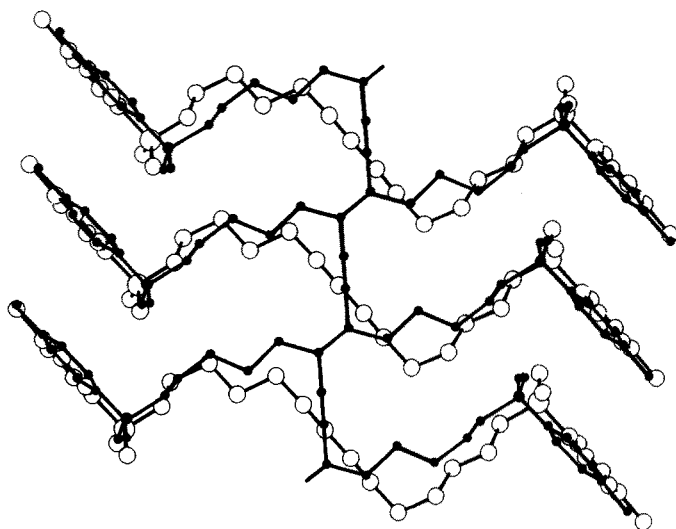


Fig. 23. Projection of the structures of PTS-12 monomer and polymer on a common plane

The unexpected behaviour can be understood if it is assumed that the terminal *p*-toluenesulfonate groups retain their position during the reaction and the entire methylene spacer is included in the rotational and translational motions. It can be seen that indeed the *p*-toluenesulfonate groups are already pseudo-centrosymmetrically related in the monomer, e.g. the center between the sulfur atoms is located at $a = 0.4989$, $b = 0.2453$ and $c = 1.0111$ which is very close to the new center of symmetry in the polymer structure. Therefore, the additional centers of symmetry which appear at the phase transition are created without much change of the side group packing only by conformational rearrangement of the methylene spacer. It also can be seen in Fig. 23 that this rearrangement involves a small movement of the phenyl rings toward the center of the molecule which accounts for the continuous decrease of the *a*-axis in the polymer phase with increasing conversion (Fig. 22).

5.3 The Low Temperature Phase of PTS

In PTS monomers and polymers transitions into low temperature structures are observed which have attracted much attention^{36, 79)}. This structural phase transition is characterized by a doubling of the unit cell as schematically shown in Fig. 24.

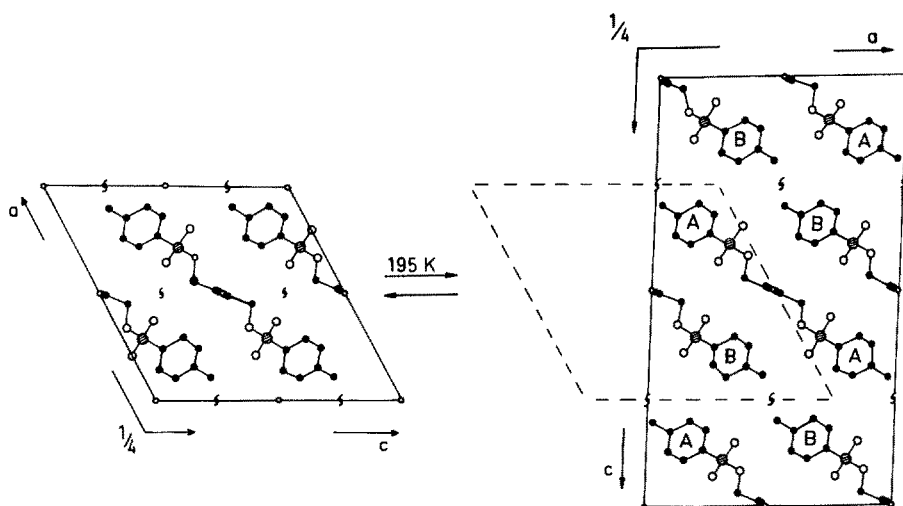


Fig. 24. Projections of the crystal structure of PTS polymer above and below the phase transition. A and B represent different side group orientations

The transition is caused by the torsion of the side groups in a manner resembling the formation of periodic stacking faults. All phenyl rings belonging to one row of molecules oriented along the (102) plane of the high temperature structure rotate by about 8 degrees in one direction, the side groups in the neighboring rows in the opposite direction. This creates crystallographically different "A" and "B" molecules in the unit cell.

Since there is only little side group reorientation the transition is connected with small anomalies of the temperature dependence of the lattice parameters (Fig. 25).

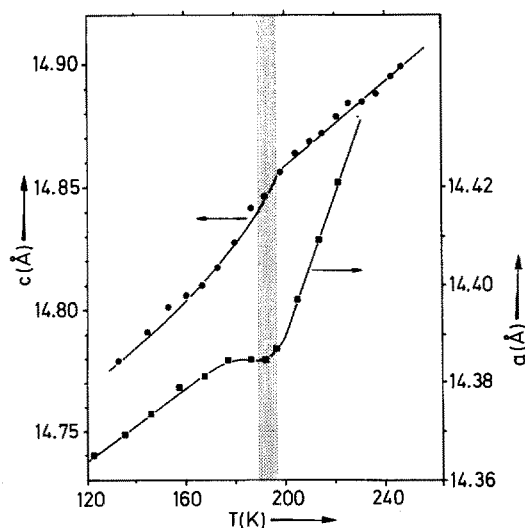


Fig. 25. Temperature dependence of the a (■) and c (●) lattice parameters of PTS polymer. The superstructure reflections appear in the shaded temperature range

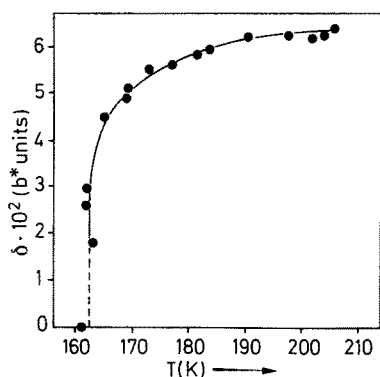


Fig. 26.

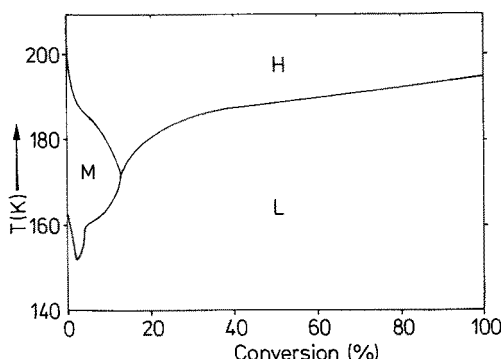


Fig. 27.

Fig. 26. Temperature dependence of the splitting δ of the satellites in the modulated PTS structure according to Ref. 95

Fig. 27. Phase diagram of PTS according to Ref. 81. H: high temperature phase, M: modulated phase, L: low temperature phase

In a small temperature range indicated in Fig. 25 additional reflections appear and all bands in the spectra begin to split into two¹¹⁸. It is interesting to note that within the experimental error the bond lengths and angles of the polymer chain stay constant in the whole temperature range and are equal in the two independent chains. The comparatively large splitting of the optical absorption of the polymer backbone ($\sim 500 \text{ cm}^{-1}$) must therefore be attributed to the small side group reorientation.

In PTS monomer and partly polymerized crystals similar transitions are observed. However, in the monomer an additional incommensurable modulated structure is present as a precursor of the low temperature structure^{81, 92–95, 119, 120}. The modulated phase is characterized by satellite reflections which appear at $0.5 a^*$, δb^* , 0 in reciprocal space, i.e. the superstructure reflections of the low temperature phase are split into two. The splitting δ in b^* direction is temperature dependent with values for δ ranging from $0.062 b^*$ at 206 K to zero at 163 K (Fig. 26). The modulated phase can be described involving an occupation probability wave of the side group orientation (molecules A and B in Fig. 24). Similar incommensurable modulated structures have been observed in other molecular crystals, e.g. in biphenyl¹²¹. The wavelength of the modulation δ^{-1} increases with decreasing temperature and finally the commensurate low temperature phase “locks in”. It is interesting to note that the incommensurable phase is absent in the polymer, probably due to the strong coupling by the polymer chain which is oriented along the modulation direction. With an increasing polymer content the temperature range in which the modulated phase is stable becomes increasingly smaller. Above a conversion of about 13 percent the transition proceeds directly from the high to the low temperature phase. The phase diagram of PTS is schematically shown in Fig. 27. In the region of the low temperature transitions a pyroelectric effect has been observed which may be interpreted differently^{122, 123}. The apparent lack of a center of symmetry stands in contrast to the space group $P2_1/c$ which is unambiguously determined by the systematic extinctions. Bloor has explained

these findings by local perturbations or macroscopic deformation of the crystal coming from the internal strain produced during polymerization ¹²³⁾.

5.4 The Low Temperature Phase of DCH

At 142 K DCH monomer undergoes a first order phase transition into an unreactive low temperature structure. The transition is accompanied by a sudden decrease of the stacking axis *b*. The crystallographic data are included in Table 3, projections of the two crystal structures are shown in Fig. 28 in comparison.

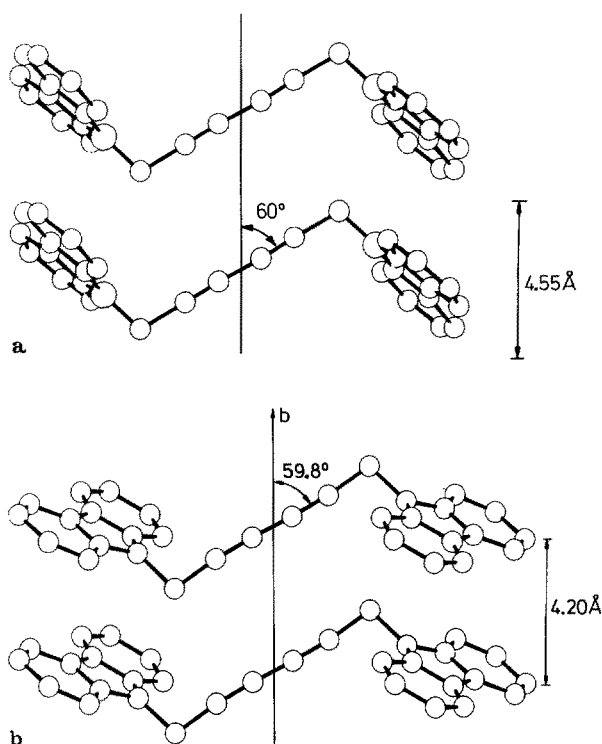
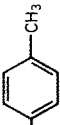
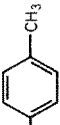
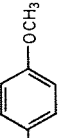
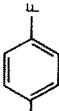
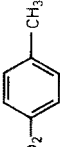
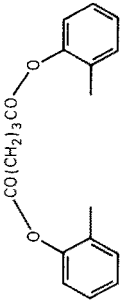



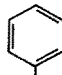
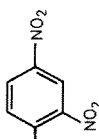

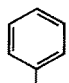
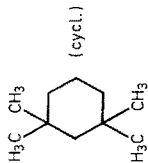


Fig. 28a and b. Crystal structures of DCH monomer above (a) and below (b) 142 K.

The phases are readily identified by the colour of polymer traces present in the crystal, blue above and red below 142 K ¹²⁴⁾. Sharp phase boundaries between the phases have been identified by Bloor et al. as the (031) and (041) crystallographic planes of the two structures. Larger crystals tend to fracture during the transition due to nucleation of several low temperature phases at crystal defects. The large change in crystal density ($\sim 4\%$) renders the transition temperature sensitive to hydrostatic pressure ^{125, 126)}. At a pressure of about $3 \cdot 10^2$ MPa the critical temperature is shifted to room temperature. This low temperature structure is not observed in DCH polymer or the anthracene substituted analogs DAH and ACH.

Table 4. Observed bond lengths of polydiacetylene chains and of butatriene model compounds

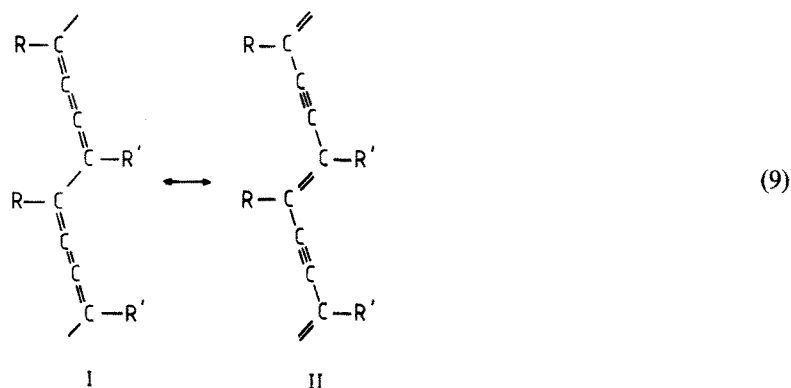
R	Abbr.	T/K	A/Å	B/Å	C/Å	Ref.
	PTS	295	1.191(4)	1.428(4)	1.356(4)	78)
	PTS	120	1.19(2)	1.43(2)	1.36(2)	79)
	MBS	295	1.195(5)	1.424(3)	1.364(5)	127)
	PFBS	295	1.17(2)	1.39(3)	1.42(3)	38)
	PTS-12	295	1.15(2)	1.41(1)	1.41(2)	42)
	BPG*	295	1.29	1.38	1.42	43, 44)
	DCH	295	1.21	1.44	1.33	84)
	DCH	295	1.23(1)	1.42(1)	1.38(1)	72, 85)

	HDU-1	295	1.21	1.42	1.36	128)
	TCDU-1	295	1.17(2)	1.38(2)	1.46(2)	83)
	DNP	295	1.205(7)	1.410(5)	1.471(9)	58)
	THD	295	1.205(2)	1.426(3) 1.427(3)	1.359(3) 1.360(3)	71)
Butatriene structure (theor.) Acetylene structure (theor.)			1.28 1.21	1.32 1.43	1.46 1.34	128) 128)
	butatriene (exp.)	100	1.259	1.348	1.478	129)
	butatriene (exp.)	295	1.261	1.332	1.547	130)

* Solid solution, 35% polymer in monomer

6 Structure of the Polydiacetylene Chain

Two different reaction mechanisms have been postulated for the topochemical polymerization of diacetylenes involving diradical or carbene chain ends ¹¹⁶⁾. The first mechanism leads to a butatriene structure (I), the latter to the acetylene structure (II) of polydiacetylene chains.



The elucidation of the reaction mechanism and the identification of the reactive intermediates has been a matter of debate and extensive studies in several laboratories; it will be covered in other reviews ¹¹⁶⁾. Sixl et al. have been able to demonstrate that the energetically favoured diradicals giving rise to the butatriene structure (I) are only observed for oligomers with comparatively short chain length ($n < 7$). In longer chains the higher energy of the carbene intermediates is overcompensated by the lower energy of the resonance structure (II) and in later stages of the reaction carbenes and dicarbenes can be identified to be the reactive chain ends. Therefore, the acetylene structure (II) is expected for the polydiacetylene chain.

The determination of bond lengths and angles of the polymer backbone is only possible in cases where the polymerization can be carried out to quantitative conversion with retention of the crystal perfection. It has been mentioned above that this condition is fulfilled in varying degrees for different reactive diacetylenes.

The experimental data for various polydiacetylenes and for two model compounds for the butatriene structure are compiled in Table 4.

It should be noted that the values given in Table 4 reflect both the different qualities of the crystal structure analyses and of the crystals. The bond lengths are not corrected for anisotropic thermal vibrations. From the differences found in two independent structure analyses of DCH polymer it can be assumed that in some cases the standard deviations given may be underestimated. In all cases the quality of the analyses does not allow the determination of the electron density distribution along the polymer chain which has been possible for the two model compounds and for the resonance structure (I) ^{129, 130)}.

Within these limits the polydiacetylene chain seems to be best represented by the acetylene structure (II). This is especially true for those polymers (PTS, HDU-1, THD) which are obtained thermally under mild conditions. In the other cases devia-

tions from the expected values can be primarily explained by defects which are introduced by γ -irradiation and in other cases by perturbations of the electron density of the polymer chain by end groups and residual monomer units. Examples for this behaviour are TCDU-1 and BPG-1 which have been claimed to represent strong admixtures of the resonance structure (I). As it has been mentioned above the polymerization of TCDU-1 is accompanied by unusually large side group rotations giving rise to large lattice changes (cf. Table 3). This introduces some disorder which is evidenced by large anisotropic thermal parameters and unusual bond lengths in the side chain ⁸³).

The second example, BPG-1, is a case of limited reactivity. The crystal structure analysis was carried out using a crystal containing only 35 percent polymer ⁴⁴). The quality of the data clearly does not allow to draw conclusions on the electronic structure of the polymer chain.

A similar argument can also be used for DNP which shows an unusually large bond length C2-C2' ("C" in Table 4). Here, the thermal polymerization is followed by a second thermally activated process leading to the destruction of the crystal ⁵⁸). This has been interpreted as a disruptive phase transition ⁹³). The unusual bond lengths can be attributed to defects introduced by the second reaction which competes with polymerization.

Resonant raman spectroscopy has proved to be another valuable tool for the study of the structure of the polydiacetylene chain. Due to the resonance enhancement the spectra are compared to greatly simplified, infrared spectra and show as principle feature only the in-plane modes of the polymer chain. The correlation of the $C\equiv C$ and $C=C$ stretching modes and their temperature dependence have been interpreted as resonances between the mesomeric structures (I) and (II) ^{131, 132}). However, a model using simple anharmonic force constants for the acetylene structure (II) is in good agreement with the experiment, e.g. the temperature and pressure dependence of the vibration frequency and the mechanical properties ¹³³⁻¹³⁵).

Many polydiacetylenes show drastic colour changes in the solid-state or in solution when the temperature or the solvent is changed ^{109-111, 114, 136-140}). This "red-to-blue" transition which is shown for one example in Fig. 29 has been interpreted in terms of different resonance contributions or changes of planarity.

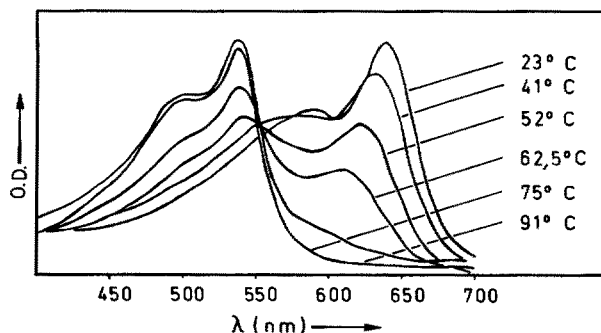


Fig. 29. Red-to-blue transition in a polydiacetylene

However, it should be emphasized at this point that despite the great effort devoted to the elucidation of this effect, which has been observed very early, to date there is no experiment which unambiguously explains the nature of the colour changes.

Two models for the shape of the polydiacetylene chain in solution are schematically presented in Fig. 30.

The first model (Kuhn chain)¹⁴¹⁾ is built up by planar segments of limited conjugation length which are separated by defects, e.g. *cis* double bonds. The second concept of a "worm-like" chain (Porod-Kratky chain)^{142, 143)} visualizes a continuous curvature of the chain skeleton. In this model the chain stiffness is characterized by the average angle between two segments or the persistence length l_{pers} . Recent studies of the solution properties of PTS-12 have shown that all data can be readily discussed in terms of the concept of "worm-like" chains.

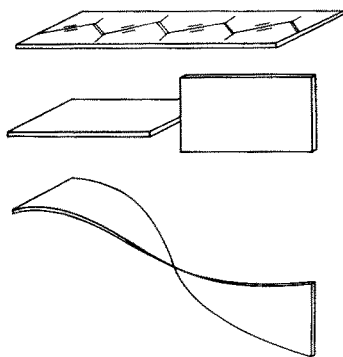


Fig. 30. Schematic representation of the shape of polydiacetylene chains. Top: planar, fully conjugated chain, middle: Kuhn model, bottom: worm-like chain

The dramatic colour changes which are observed in solutions of certain polydiacetylenes, e.g. poly3BCMU or poly4BCMU, when the solvent to non-solvent ratio or the temperature is changed, have been interpreted as single-chain coil-to-rod transition^{109–111, 144, 145)}. However, this is still a matter of debate and continuing experiments. There is experimental evidence that this transition is connected with an aggregation process^{114, 146)}.

In conclusion it must be admitted that the spectral changes of polydiacetylene chains in various environments, which are intimately coupled to the electronic structure of the backbone, are still not fully understood and remain one of the unsolved problems in this field.

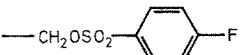
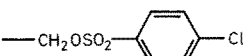
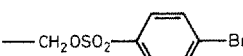
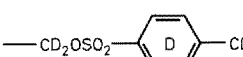
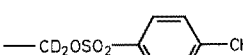
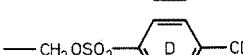


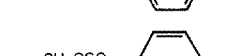


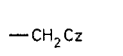
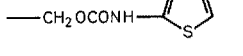
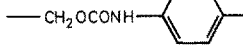
7 Polymerization in Mixed Crystals

Owing to the special principles of topochemical reactions polydiacetylene copolymers can only be obtained if the comonomers form mixed crystals. Apart from this obvious preparative aspect mixed crystals are of interest because it can be expected that the monomer reactivity and the polymer properties can be effectively varied by the crystal composition. Similar effects have been successfully demonstrated in the "isostructural doping" of organic charge-transfer crystals¹⁴⁷⁾. In addition, it can be

imagined that comonomer units introduced into the host lattice can be regarded as well defined defect sites. These could be used as probes in order to obtain further insight into the complex energy transfer processes during the reaction.

A necessary and sufficient condition for the formation of substitutional solid solutions of organic molecules is similarity of shape and size of the component molecules. For the formation of a continuous series of solid solutions the crystal structures of the pure components must be isomorphous¹⁴⁸⁾. Due to the rather irregular shape of organic molecules the principle of close packing leads to structures of low symmetry so that the latter requirement is not often fulfilled. Several diacetylenes which were found to form mixed crystals are given in Table 5. A large number of

Table 5. Diacetylene monomers forming mixed crystals
A: anthryl group, Cz: carbazolyl group

Monomer 1	Monomer 2 R	R'	Ref.
PTS		= R	38)
PTS		= R	149,150)
PTS		= R	150)
PTS		= R	88,89)
PTS		= R	88,89)
PTS		= R	88,89)
PTS	¹³ 	= R	88,89)
PTS		= R	151)
PTS		= R	151)
DCH		= R	48)
DCH			48)
H DU - 1		= R	152)
H DU - 1		= R	153)

comonomers forming mixed crystals with PTS have been obtained by chemical modification of the p-toluenesulfonate side group. Of these only the various deuterated and ^{13}C labelled compounds as well as PFBS form mixed crystals over the whole concentration range. The isotope labelled compounds form ideal solid solutions in the PTS matrix and consequently all properties, e.g. the kinetic isotope effects change accordingly to the comonomer content.

PFBS ($\text{R} = -\text{CH}_2-\text{OSO}_2-\text{C}_6\text{H}_4-\text{F}$) crystallizes in a structure which is isomorphous

to PTS and exhibits virtually identical packing parameters. However, thermal polymerization proceeds much slower and by changing the crystal composition the reactivity can be changed by a factor of 8^{38,154}. Time conversion curves are shown in Fig. 31. The PFBS comonomer acts as a lattice site where the chain termina-

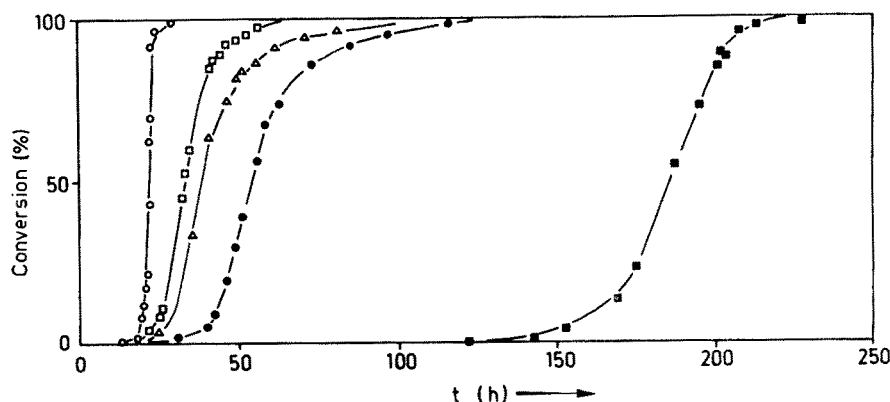


Fig. 31. Time conversion curves for the thermal polymerization of PTS-PFBS mixed crystals at 60 °C. ○: PTS, ■: PFBS, □: 20 mole % PFBS, △: 50 mole % PFBS, ●: 62 mole % PFBS

tion probability is greatly enhanced. Since the rapid reaction regime has much higher kinetic chain lengths it is affected by much smaller admixture of the comonomer than the reaction in the induction period. The kinetic data are plotted in Fig. 32.

The other comonomers for PTS given in Table 5 form mixed crystals only in a limited concentration range. In contrast to PBS the chloro and bromo derivatives PCS and PBS form completely unreactive triclinic structures (cf. Table 1). However, by crystallization of these monomers at very high supersaturations crystals of metastable reactive modifications are obtained which have been shown to be isomorphous to PTS¹⁵⁰. Owing to the crystallization conditions these crystals are unfortunately not suited for detailed structural investigations. The metastable phases melt up to 50 degrees below the stable modifications which spontaneously recrystallize from the melt.

When PCS and PBS are cocrystallized with PTS two sorts of mixed crystals are formed simultaneously, i.e. active crystals in which up to 20 percent of PCS can be incorporated in the PTS lattice and inactive crystals where PTS is dissolved in the comonomer structure. The cocrystallization diagram for the system PTS-PCS is shown in Fig. 33.

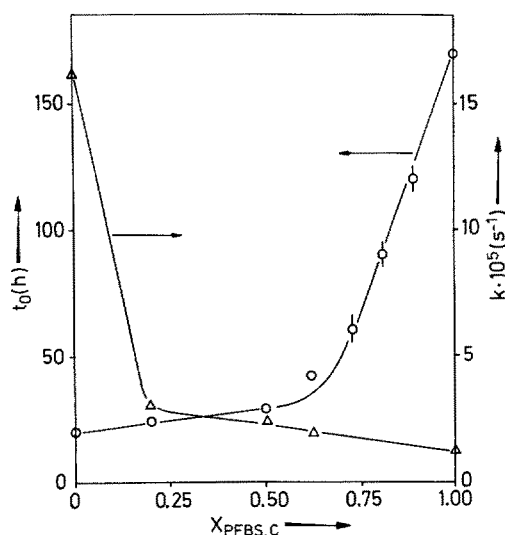


Fig. 32. Dependence of the induction period t_0 and the first order rate constant k of the rapid reaction for the data plotted in Fig. 31

The dependence of crystal reactivity is rather complicated. At small admixtures ($x_{\text{PCS}} < 0.05$) the induction period is decreased but at higher concentrations substantially increased.

It is interesting to note that the transition into the low temperature phases is inhibited by the replacement of a relatively small number of terminal methyl groups. It seems that the phase transition is mediated by interactions of the methyl groups. Replacement of about 10 percent of the methyl groups by fluorine is sufficient to suppress the transition below 110 K although the free volume associated with the methyl group rotation is retained³⁸. In the more closely packed polymer this effect is even more

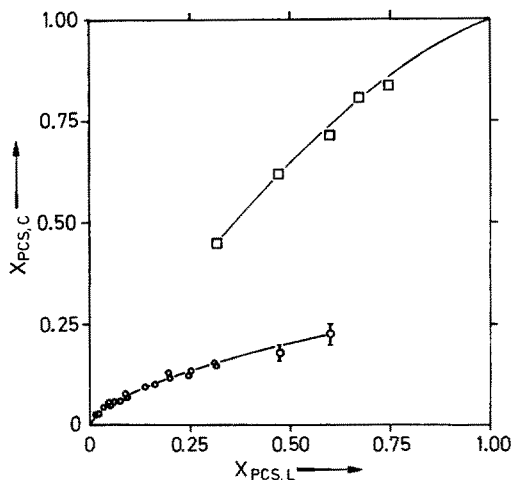


Fig. 33. Cocrystallization diagram for the crystallization of PTS-PCS mixed crystals. $x_{\text{PCS,L}}$, $x_{\text{PCS,C}}$ are mole fractions of PCS in the acetone solution and in the mixed crystals

pronounced. Pure PFBS monomer and polymer show no phase transition down to 4.2 K^{155, 156}). The other diacetylene monomer which is known to form substitutional mixed crystals over the whole concentration range is DCH. The anthracene rings in the comonomer DAH and ACH are able to replace the carbazolyl groups. This is demonstrated by the fact that ACH forms an order-disorder structure which is isomorphous to DCH and in which both side groups statistically occupy the same lattice sites. Owing to the closer packing DAH and ACH are completely inactive (cf. Table I).

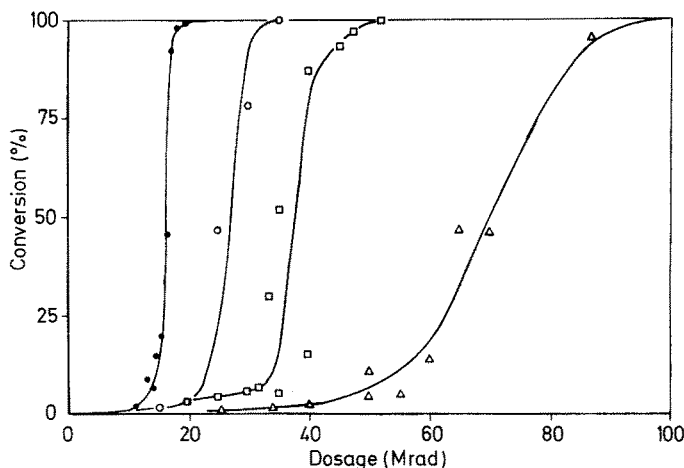


Fig. 34. Dosage conversion curves for the γ -ray polymerization of DCH-ACH mixed crystals. ●: DCH, ○: 1.1 mole % ACH, □: 2.2 mole % ACH, △: 5.5 mole % ACH

The admixture of small amounts of anthracene containing comonomers has a drastic effect on the polymerization rate (Fig. 34). In crystals containing 2 percent ACH the induction period is more than doubled. This cannot be explained by the monomer packing since the lattice parameters are virtually unchanged in this composition range. It is also not probable that the comonomer would act as a chain-terminating impurity since in the induction period the kinetic chain length is much smaller than the average distance between two comonomer units.

Two explanations for this behaviour are possible. First, the anthracene rings inhibit phase transition which is necessary in order to bring about high reactivity. In pure DAH and ACH the phase transitions which have been described for DCH are absent.

Secondly, it has been proposed that the anthryl groups act as traps for the excited states which are formed in the first stage of photopolymerization so that most of the energy is emitted as fluorescence before it is transferred to the triple bond system.

If these mixed crystals are irradiated, however, at 400 nm where only the anthryl groups absorb a small photosensitization can be observed. Neither of the two models have been fully established experimentally to date.

8 References

1. Baeyer, A., Landsberg, L.: *Ber. dt. chem. Ges.* 15, 61 (1884)
2. Baeyer, A., Bloem, L.: *Ber. dt. chem. Ges.* 17, 964 (1886)
3. Castille, A.: *Bull. Acad. Roy. Med. Belg.* 6, 152 (1941)
4. Dunitz, J. D., Robinson, J. M.: *J. Chem. Soc.* 1947, 1145
5. Bowden, K., Heilbron, I., Jones, E. R. H., Sargeant, K. H.: *J. Chem. Soc.* 1947, 1579
6. Armitage, J. B. A., Cook, C. L., Entwistle, N., Jones, E. R. H., Whiting, M. C.: *J. Chem. Soc.* 1952, 1998
7. Bohlmann, F.: *Ber. dt. chem. Ges.* 84, 785 (1951)
8. Black, H. K., Weedon, B. C. L.: *J. Chem. Soc.* 1953, 1785
9. Seher, A.: *Liebigs Ann. Chem.* 589, 222 (1954)
10. Bohlmann, F.: *Angew. Chem.* 69, 82 (1957)
11. Hirshfeld, F. L., Schmidt, G. M. J.: *J. Polym. Sci. A* 2, 2181 (1964)
12. Wegner, G.: *Z. Naturforsch. (b)* 24, 824 (1969)
13. Schmidt, G. M. J.: *Solid state photochemistry*. Weinheim: Verlag Chemie 1976
14. Liebermann, C.: *Ber. dt. chem. Ges.* 22, 124 (1889); 22, 782 (1889)
15. Wegner, G.: Recent progress in the chemistry and physics of poly (diacetylenes). In: *Molecular metals*. Hatfield, W. E. (ed.). New York: Plenum Press 1979, pp. 209–242
16. Bloor, D.: *Springer Lect. Notes in Phys.* 113, 14 (1980)
17. Baughman, R. H., Chance, R. R.: *Ann. N.Y. Acad. Sci.* 313, 705 (1978)
18. Wegner, G.: Organic linear polymers with conjugated double bonds. In: *Chemistry and physics of one-dimensional metals*. Keller, H. J. (ed.). New York: Plenum Press 1977, pp. 297–314
19. Wegner, G.: *Pure and Appl. Chem.* 49, 443 (1977)
20. Wegner, G.: *Faraday Disc.* 68, 494 (1980)
21. Enkelmann, V.: *Springer Lect. Notes in Phys.* 113, 1 (1980)
22. Baughman, R. H.: *J. Polym. Sci., Polym. Phys. Ed.* 12, 1511 (1974)
23. Baughman, R. H., Yee, K. C.: *J. Polym. Sci., Macromol. Rev.* 13, 219 (1978)
24. Enkelmann, V.: *Coll. and Polym. Sci.* 256, 893 (1978)
25. Bloor, D.: The polymerization of disubstituted diacetylene crystals. In: *Developments in crystalline polymers*. Bassett, D. C. (ed.). Barking: Applied Science Publishers 1982, pp. 151–193
26. Wegner, G., Fischer, E. W., Munoz-Escalona, A.: *Makromol. Chem. Suppl.* 1, 521 (1975)
27. Penzien, K., Schmidt, G. M. J.: *Angew. Chem. Int. Ed.* 8, 608 (1969)
28. Elgavi, A., Green, B. S., Schmidt, G. M. J.: *J. Amer. Chem. Soc.* 95, 2058 (1973)
29. Green, B. S., Lahav, M., Rabinovich, D.: *Acc. Chem. Res.* 12, 191 (1979)
30. Baughman, R. H., Chance, R. R., Cohen, M. J.: *J. Chem. Phys.* 64, 1869 (1976)
31. Kaiser, J., Wegner, G., Fischer, E. W.: *Israel J. Chem.* 10, 157 (1972)
32. Meyer, W., Lieser, G., Wegner, G.: *Makromol. Chem.* 178, 631 (1977); *J. Polym. Sci., Polym. Phys. Ed.* 16, 1365 (1978)
33. Braun, H. G., Wegner, G.: *Mol. Cryst. Liq. Cryst.* 96, 121 (1983); Braun, H. G., Enkelmann, V.: *Acta Cryst. C*, submitted
34. Wegner, G., Enkelmann, V.: *Angew. Chem.* 89, 432 (1977)
35. Enkelmann, V., Leyrer, R. J., Wegner, G.: *Makromol. Chem.* 180, 1787 (1979)
36. Enkelmann, V., Wegner, G.: *Makromol. Chem.* 178, 635 (1977)
37. Mayerle, J. J., Clarke, T. C.: *Acta Cryst. B* 34, 143 (1978)
38. Enkelmann, V.: *Makromol. Chem.* 184, 1945 (1983)
39. Fisher, D. A., Ando, D. J., Bloor, D., Hursthouse, M. B.: *Acta Cryst. B* 35, 2075 (1979)
40. Williams, R. L., Ando, D. J., Bloor, D., Hursthouse, M. B.: *Acta Cryst. B* 35, 2075 (1979)
41. Williams, R. L., Ando, D. J., Bloor, D., Hursthouse, M. B., Motevalli, M.: *Acta Cryst. B* 36, 2155 (1980)
42. Siegel, D., Sixl, H., Enkelmann, V., Wenz, G.: *Chem. Phys.* 72, 201 (1982)
43. Lando, J. B., Day, D., Enkelmann, V.: *Polym. Symp.* 65, 73 (1978)
44. Day, D., Lando, J. B.: *J. Polym. Sci., Polym. Phys. Ed.* 16, 1009 (1978)
45. Enkelmann, V., Graf, H. J.: *Acta Cryst. B* 34, 3715 (1978)
46. Mayerle, J. J., Flandera, M. A.: *Acta Cryst. B* 34, 1374 (1978)
47. Enkelmann, V., Schleier, G., Wegner, G., Eichele, H., Schwoerer, M.: *Chem. Phys. Lett.* 52, 314 (1977)

48. Enkelmann, V., Schleier, G., Eichele, H.: *J. Mater. Sci.* **17**, 533 (1982)
49. Kaiser, J.: Dissertation. Mainz: 1972
50. Enkelmann, V.: *J. Chem. Res. (S)* **1981**, 344; *J. Chem. Res. (M)* **1981**, 3901
51. Gross, H., Sixl, H., Kröhnke, C., Enkelmann, V.: *Chem. Phys.* **45**, 15 (1980)
52. Patel, G. N., Duesler, E. N., Curtin, D. Y., Paul, I. C.: *J. Amer. Chem. Soc.* **102**, 461 (1980)
53. Hädicke, E., Penzien, K., Schnell, H. W.: *Angew. Chem.* **83**, 1024 (1971)
54. Fisher, D. A., Ando, D. J., Batchelder, D. N., Hursthouse, M. B.: *Acta Cryst. B* **34**, 3799 (1978)
55. Fisher, D. A., Batchelder, D. N., Hursthouse, M. B.: *Acta Cryst. B* **34**, 2365 (1978)
56. Morosin, B., Harrah, L.: *Acta Cryst. B* **33**, 1760 (1977)
57. Hanson, A. W.: *Acta Cryst. B* **31**, 831 (1975)
58. McGhie, A. R., Lipscomb, G. F., Garito, A. F., Desai, K. N., Kalyanaraman, P. S.: *Makromol. Chem.* **182**, 965 (1981)
59. Wibenga, E. H.: *Z. Kristallogr.* **102**, 193 (1940)
60. Mayerle, J. J., Clarke, T. C., Bredfeldt, K.: *Acta Cryst. B* **35**, 1519 (1979)
61. Jeffrey, G. A., Rollet, J. S.: *Proc. Roy. Soc. A* **213**, 86 (1952)
62. Brouty, C., Spinat, P., Whuler, A.: *Acta Cryst. B* **36**, 2624 (1980)
63. Enkelmann, V., Schleier, G.: *Acta Cryst. C*, in press
64. Enkelmann, V., Schleier, G.: *Acta Cryst. C*, in press
65. Williams, R. L., Ando, D. J., Bloor, D., Motevalli, M., Hursthouse, M. B.: *Acta Cryst. B* **38**, 2078 (1982)
66. Enkelmann, V., Wenz, G., Müller, M. A., Schmidt, M., Wegner, G.: *Mol. Cryst. Liq. Cryst.* in press
67. Spinat, P., Whuler, A., Brouty, C.: *Acta Cryst. C* **39**, 1084 (1983)
68. Brouty, C., Spinat, P., Whuler, A.: *Acta Cryst. C* **39**, 594 (1983)
69. Coles, B. F., Hitchcock, P. B., Walton, D. R. M.: *J. Chem. Soc. Dalton* **1975**, 442
70. Enkelmann, V., Schleier, G.: unpublished results
71. Enkelmann, V., Schleier, G.: *Acta Cryst. B* **36**, 1954 (1980)
72. Enkelmann, V., Kröhnke, C.: unpublished results
73. Enkelmann, V., Wenz, G.: unpublished results
74. Tieke, B., Bloor, D.: *Makromol. Chem.* **182**, 133 (1981)
75. Tieke, B., Bloor, D., Young, R. J.: *J. Mater. Sci.* **17**, 1156 (1982)
76. Galiotis, C., Young, R. J., Ando, D. J., Bloor, D.: *Makromol. Chem.*, in press
77. Kiji, J., Kaiser, J., Wegner, G., Schulz, R. C.: *Polymer* **14**, 433 (1973)
78. Kobelt, D., Paulus, E. F.: *Acta Cryst. B* **30**, 232 (1974)
79. Enkelmann, V.: *Acta Cryst. B* **33**, 2842 (1977)
80. Bloor, D., Koski, L., Stevens, G. C., Preston, F. H., Ando, D. J.: *J. Mater. Sci.* **10**, 1678 (1975)
81. Aimé, J. P.: Thèse. Orsay: 1983
82. Lando, J. B.: private communication
83. Enkelmann, V., Lando, J. B.: *Acta Cryst. B* **34**, 2352 (1978)
84. Apgar, P. A., Yee, K. C.: *Acta Cryst. B* **34**, 957 (1978)
85. Enkelmann, V.: Habilitationsschrift. Freiburg: 1983
86. Wegner, G.: *Makromol. Chem.* **154**, 35 (1972)
87. Garito, A. F., McGhie, A. R., Kalyanaraman, P. S.: Kinetics of solid state polymerization of 2,4-hexadiyne-1,6-diol bis (p-toluene sulfonate). In: *Molecular metals*. Hatfield, W. E. (ed.). New York: Plenum Press 1979, pp. 255–260
88. Kröhnke, C.: Dissertation. Freiburg: 1979
89. Kröhnke, C., Enkelmann, V., Wegner, G.: *Chem. Phys. Lett.* **71**, 38 (1980)
90. Patel, G. N., Chance, R. R., Turi, E. A., Khanna, Y. P.: *J. Amer. Chem. Soc.* **100**, 6644 (1978)
91. Grimm, H., Axe, D., Kröhnke, C.: *Phys. Rev. B* **25**, 1709 (1982)
92. Robin, P.: Thèse. Orsay: 1980
93. Albouy, P. A.: Thèse. Orsay: 1982
94. Albouy, P. A., Patillon, P. A., Pouget, J. P.: *Mol. Cryst. Liq. Cryst.* **95**, 239 (1983)
95. Robin, P., Pouget, J. P., Comes, R., Moradpour, A.: *J. de Phys.* **41**, 415 (1980)
96. Bloor, D., Kennedy, R. J., Batchelder, D. N.: *J. Polym. Sci., Polym. Phys. Ed.* **17**, 1355 (1979)
97. Batchelder, D. N., Bloor, D.: *J. Polym. Sci., Polym. Phys. Ed.* **17**, 569 (1979)
98. Voigt, W.: *Lehrbuch der Kristallphysik*. Berlin: Teubner 1910
99. Reuss, A.: *Angew. Math. Mech.* **9**, 49 (1929)

100. Holliday, L.: *Composite Materials*. New York: Elsevier 1966
101. Leyrer, R. J., Wettling, W., Wegner, G.: *Ber. Bunsenges. Phys. Chem.* **84**, 880 (1980)
102. Baughman, R. H.: *J. Chem. Phys.* **68**, 3110 (1978)
103. Lochner, K., Hinrichsen, T., Wolfberger, W., Bässler, H.: *Phys. stat. sol. (a)* **50**, 95 (1978)
104. Lochner, K., Bässler, H., Hinrichsen, T.: *Ber. Bunsenges. Phys. Chem.* **83**, 899 (1979)
105. Bloor, D., Ando, D. J., Hubble, C. L., Williams, R. L.: *J. Polym. Sci., Polym. Phys. Ed.* **18**, 779 (1980)
106. Bloor, D., Ando, D. J., Fisher, D. A., Hubble, C. L.: Solid state reactivity of some bis (aromatic sulphonate) diacetylenes. In: *Molecular metals*. Hatfield, W. E. (ed.). New York: Plenum Press 1979, pp. 249–253
107. Bässler, H.: *Adv. Polym. Sci.*, in press
108. Baughman, R. H., Chance, R. R.: *J. Chem. Phys.* **73**, 4113 (1980)
109. Patel, G. N.: *J. Polym. Sci., Polym. Lett. Ed.* **16**, 607 (1978)
110. Patel, G. N., Chance, R. R., Witt, J. D.: *J. Chem. Phys.* **70**, 4387 (1979)
111. Patel, G. N., Walsh, E. K.: *J. Polym. Sci., Polym. Lett. Ed.* **17**, 203 (1979)
112. Wenz, G., Wegner, G.: *Makromol. Chem., Rapid Commun.* **3**, 231 (1982); *Mol. Cryst. Liq. Cryst.* **96**, 99 (1983)
113. Plachetta, C., Schulz, R. C.: *Makromol. Chem., Rapid Commun.* **3**, 815 (1982)
114. Wenz, G., Müller, M. A., Schmidt, M., Wegner, G.: *Polymer*, in press
115. Wenz, G.: *Dissertation*. Freiburg: 1983
116. Sixl, H.: *Adv. Polym. Sci.*, in press
117. Enkelmann, V., Leyrer, R. J., Schleier, G., Wegner, G.: *J. Mater. Sci.* **15**, 168 (1980)
118. Bloor, D., Preston, F. H.: *Phys. stat. sol. (a)* **39**, 607 (1977)
119. Robin, P., Pouget, J. P., Comes, R., Moradpour, A.: *Chem. Phys. Lett.* **71**, 217 (1980)
120. Fukui, M., Sumi, S., Hatta, I., Abe, R.: *Jap. J. Appl. Phys.* **19**, L 559 (1980)
121. Cailleau, H., Moussa, F., Mons, J.: *Solid State Comm.* **31**, 521 (1979)
122. Kiess, H., Clarke, R.: *Phys. stat. sol. (a)* **49**, 133 (1978)
123. Xiao, D. Q., Ando, D. J., Bloor, D.: *Mol. Cryst. Liq. Cryst.* **95**, 201 (1983)
124. Kennedy, R. J., Chalmers, I. F., Bloor, D.: *Makromol. Chem., Rapid Commun.* **1**, 357 (1980)
125. Lacey, R. J., Williams, R. L., Kennedy, R. J., Bloor, D., Batchelder, D. N.: *Chem. Phys. Lett.* **83**, 65 (1981)
126. Bloor, D., Chalmers, I. F., Kennedy, R. J., Motevalli, M.: *Mol. Cryst. Liq. Cryst.* **95**, 215 (1983)
127. Williams, R. L., Ando, D. J., Bloor, D., Hursthouse, M. B.: *Polymer* **21**, 1269 (1980)
128. Hädicke, E., Mez, E. C., Krauch, C. H., Wegner, G., Kaiser, J.: *Angew. Chem.* **83**, 253 (1971)
129. Berkovitch-Yellin, Z., Leiserowitz, L.: *J. Amer. Chem. Soc.* **97**, 5627 (1975); *Acta Cryst. B* **33**, 3657 (1977)
130. Irngartinger, H., Jäger, H. U.: *Angew. Chem.* **88**, 615 (1976)
131. Melveger, A. J., Baughman, R. H.: *J. Polym. Sci., Polym. Phys. Ed.* **11**, 603 (1973)
132. Baughman, R. H., Witt, J. D., Yee, K. C.: *J. Chem. Phys.* **60**, 4755 (1974)
133. Lewis, W. F., Batchelder, D. N.: *Chem. Phys. Lett.* **60**, 232 (1979)
134. Cottle, A. C., Lewis, W. F., Batchelder, D. N.: *J. Phys. C* **11**, 605 (1978)
135. Mitra, V. K., Risen, Jr., W. M., Baughman, R. H.: *J. Chem. Phys.* **66**, 2731 (1977)
136. Chance, R. R., Baughman, R. H., Müller, H., Eckhardt, C. J.: *J. Chem. Phys.* **67**, 3616 (1977)
137. Iqbal, Z., Chance, R. R., Baughman, R. H.: *J. Chem. Phys.* **66**, 5520 (1977)
138. Exarhos, G. J., Risen, Jr., W. M., Baughman, R. H.: *J. Amer. Chem. Soc.* **98**, 481 (1976)
139. Boudreaux, D. S., Chance, R. R.: *Chem. Phys. Lett.* **51**, 273 (1977)
140. Bloor, D., Hubble, C. L.: *Chem. Phys. Lett.* **56**, 89 (1978)
141. Kuhn, H.: *Fortschr. Chem. Org. Naturstoffe* **16**, 169 (1958); **17**, 404 (1959)
142. Porod, G.: *Monatsh. Chem.* **80**, 251 (1949)
143. Kratky, O., Porod, G.: *Rec. Trav. Chim.* **68**, 1106 (1949)
144. Lim, K. C., Fincher, L. H., Heeger, A. J.: *Phys. Rev. Lett.* **50**, 1934 (1983)
145. Berlinsky, A. J., Wudl, F., Lim, K. C., Fincher, C. R., Heeger, A. J.: Theory of the rod-to-coil transition in polydiacetylene. Preprint 1983; *Mol. Cryst. Liq. Cryst.*, in press
146. Müller, M. A., Schmidt, M., Wegner, G.: *Makromol. Chem., Rapid Commun.*, in press

147. Tomkiewicz, Y., Engler, E. M., Scott, B. A., La Placa, S. J., Brom, H.: Doping organic solids — its uses to probe and to modify electronic properties. In: Molecular metals. Hatfield, W. E. (ed.). New York: Plenum Press 1979, pp. 43–49
148. Kitaigorodskii, A. I.: Molecular crystals and molecules. New York: Academic Press 1973
149. Enkelmann, V.: Makromol. Chem. 179, 2811 (1978)
150. Enkelmann, V.: J. Mater. Sci. 15, 951 (1980)
151. Ando, D. J., Bloor, D., Tieke, B.: Makromol. Chem., Rapid Commun. 1, 385 (1980)
152. Kröhnke, C.: Diplomarbeit. Freiburg: 1977
153. Patel, G. N., Miller, G. G.: Copolymerization of diacetylenes in the crystalline solid state — a method for recording latent finger prints. Preprint: 1976
154. Yee, K. C.: J. Org. Chem. 44, 2571 (1979)
155. Sixl, H.: private communication
156. Chance, R. R., Yee, K. C., Baughman, R. H., Eckhardt, H., Eckhardt, C. J.: J. Polym. Sci., Polym. Phys. Ed. 18, 1651 (1980)

H.-J. Cantow (Editor)

Received January 18, 1984